Tectonophysics
November 2022, Volume 842, Pages 229592 (21p.)
https://doi.org/10.1016/j.tecto.2022.229592
https://archimer.ifremer.fr/doc/00796/90832/

Volcanic influence during the formation of a transform marginal plateau: Insights from wide-angle seismic data along the northwestern Demerara Plateau

Padron Mora Crelia [1, 2], Klingelhoefer Frauke [2, *], Roest Walter [2], Graindorge David [3], Loncke Lies [4], Basile Christophe [5], Sapin François [6], Lesourd-Laux Thomas [2], Museur Thomas [2], The Margats Team

[1] Departamento de Ciencias de la Tierra, Universidad Simón Bolívar (USB), Caracas, Venezuela
[2] Geo-Ocean, Ifremer, ZI de la Pointe de Diable, CS 10070, 29280 Plouzané, France
[3] Geo-Ocean, Université de Brest, Institut Universitaire Européen de la Mer, rue Dumont Durville, 29280 Plouzané, France
[4] Univ. Perpignan Via Domitia, Centre de Formation et de Recherche sur les Environnements Méditerranéens (CEFREM), UMR 5110, 52 Avenue Paul Alduy, 66860 Perpignan, France
[5] Univ. Grenoble Alpes, Univ. Savoie Mont Blanc, CNRS, IRD, IFSTTAR, ISTerre, 38000, France
[6] TotalEnergies SE, Centre Scientifique et Technique Jean Feger (CSTJF), Avenue Larribau, 64018 Pau, France

* Corresponding author : Frauke Klingelhoefer, email address : fklingel@ifremer.fr

Abstract :

Transform marginal plateaus (TMPs) are submarine seafloor highs located at the continental slope, often at the boundary of two ocean basins of different ages and associated to at least one transform or highly oblique margin. The systematic study of TMPs can, therefore, answer questions about rifting and continental margin development. The Demerara TMP (offshore Suriname and French Guiana) is located at the border between the Central Atlantic, which opened during the Lower Jurassic and the Equatorial Atlantic, which opened during the Lower Cretaceous. This study, based on wide-angle seismic data modeling from the northern and western section of the Demerara Plateau, provides information on both the lower volcanic unit of this TMP and the adjacent oceanic crust. The results confirm that the crust of the Demerara Plateau is around 30 km thick and consists of lava flows possibly mixed with crust of continental origin in its deeper layers. Seismic velocities (exceeding 7 km/s) are compatible with those of volcanic oceanic plateaus. To the west, a relatively wide transition zone separates the plateau from the Jurassic oceanic crust, which is composed of two layers, and is much thicker than normal oceanic crust (~11 km). During the Cretaceous, the plateau was sharply cut by transform and highly oblique structures, separating the Demerara Plateau from its transform conjugate, the Guinea Plateau. As a result, the Demerara Plateau is flanked to the north by a magma-poor/strongly tectonized Cretaceous oceanic domain with thin (2–3 km) crust, likely partially consisting of serpentinized mantle. In contrast, the oceanic crust located towards the south-east appears to be more characteristic of typical oceanic crust in composition though slightly thinner than normal (4–6 km) thickness. Our analysis allows us to propose a new 3D vision of the crustal structure of the Demerara TMP and its borders.

Highlights

► Processing and interpretation of wide-angle and multi-channel reflection seismic data confirm the volcanic origin of the Demerara transform marginal plateau located offshore French Guiana and Surinam. ► The Jurassic Central Atlantic oceanic crust located to the west of the Demerara Plateau is much thicker than normal oceanic crust. ► The northern margin of the Demerara Plateau is characterised by an abrupt transition zone, typical for transform or highly oblique continental margins. ► To the north of the Demerara Plateau, Equatorial Atlantic crust of Cretaceous origin is relatively thin and its velocity structure compatible with that of serpentinised upper mantle.

Keywords : Dermerara Plateau, Wide-angle seismics, Volcanic margins, Equatorial Atlantic

1 Introduction

Transform Marginal Plateaus (TMPs) are submarine seafloor highs located deeper than the shelf break, often located at the boundary of two oceanic basins of different ages (Mercier de Lepinay, 2016; Loncke et al., 2020). By definition, one side of the plateau is associated with a transform or highly oblique margin (Loncke et al., 2020). Thus, their formation seems to be directly related to the timing and mechanism of the rifting processes. Most TMPs comprise abundant magmatic material, indicating the influence of a mantle thermal anomaly during their construction. Only few are underlain by pure continental crust (Loncke et al., 2020; Museur et al., 2021). However, the mechanisms at the origin of their formation are still poorly understood. Main unsolved questions are if all TMPs have undergone at least one volcanic phase and how the ratio of original crust and magmatic products vary between TMPs. Their role in the formation of transform margins can only be understood once the internal structure of the TMPs is known. By their position TMPs might also have been last land bridges between continents at the opening of neighboring ocean basins, again a question which can only be solved once the lithology, crustal nature, volcanic imprint and sedimentary structures are sufficiently known on conjugate TMPs. Bringing new observations from the Demerara Plateau (Figure 1), this study hopes to contribute to a better understanding of the formation of TMPs and therefore assists in answering questions about rift propagation, and the relation between transform margin initiation and volcanic activity (Burke and Dewey, 1973; Basile et al., 2020; Loncke et al., 2020).

The Demerara Plateau at the connection between the Central and the Equatorial Atlantic Basins and its conjugate, the Guinea Plateau, formed during two phases. Their western border formed during the opening of the Central Atlantic during the Jurassic as a rifted volcanic margin conjugate to the Bahamas plateau (Nemcok, 2016; Reuber et al., 2016; Museur et al., 2021). Basile et al. (2020) associate the discovery of 173.4 Ma magmatic rocks at the northern edge of the Demerara Plateau with the formation of the Jurassic margin under the influence of a hotspot. At the end of the Jurassic, Demerara and Guinea plateaus were contiguous (Loncke et al., 2020, Casson et al., 2021; Loncke et al., 2022). The northern border of Demerara (and the southern border of the conjugate Guinea Plateau) formed during the Cretaceous as a transform margin (Gouyet, 1988; Campan, 1995; Greenroyd et al., 2007; Basile et al., 2013; Mercier de Lépinay, 2016, Basile et al., 2020) and its eastern border represent a Cretaceous rifted margin (Basile et al., 2013; Sapin et al., 2016; Museur et al., 2021).

To shed light on the deep structure of the Demerara Plateau a deep-sounding wide-angle seismic survey was carried out in 2016 (Graindorge and Klingelhoefer, 2016). The objectives were to answer questions on the nature and structure of the plateau and the surrounding oceanic crust and on the formation of TMPs in general. Results from the eastern domain of the plateau were presented by Museur et al., 2021 and this study focuses on the western domain of the plateau.

2 Previous work

Early seismic exploration of the Demerara Plateau was mostly undertaken for the purpose of hydrocarbon exploration and did not penetrate to the lower layers of the edifice (e.g. Gouyet et al., 1994). Sonobuoy wide-angle seismic profiles were acquired in the region; however, they constrained seismic velocities down to the upper crust only (Edgar & Ewing, 1968; Houtz, 1977; Houtz et al., 1977). From these, a sedimentary origin of the Demerara rise was

proposed with the plateau consisting of sediments prograding the continental shelf by 150 km (Edgar & Ewing, 1968).

One of the first modern deep sounding experiments along the Demerara Plateau was conducted in the scope of the Amazon Cone Experiment (Greenroyd et al., 2007; Greenroyd et al., 2008). Profile D (Figure 1), which spanned the complete plateau, imaged a 35-37 km thick crust close to the shore line, thinning seaward to 10-11 km over a distance of 320 km. Offshore, the oceanic crust along the profile was found to be 3.3-5.7 km thick, thus thinner than normal oceanic crust (White et al., 1992), but typical for oceanic crust affected by long-lived transform faults or formed at slow spreading ridges (Van Avendonk et al., 2001; Bown and White, 1994). The plateau itself was interpreted to consist of thinned continental crust (Greenroyd et al., 2008). However, in that study a significant part the plateau itself was not covered by wide-angle seismic instruments due to the shallow water depth, probably complicating the precise definition of the internal structure of the plateau.

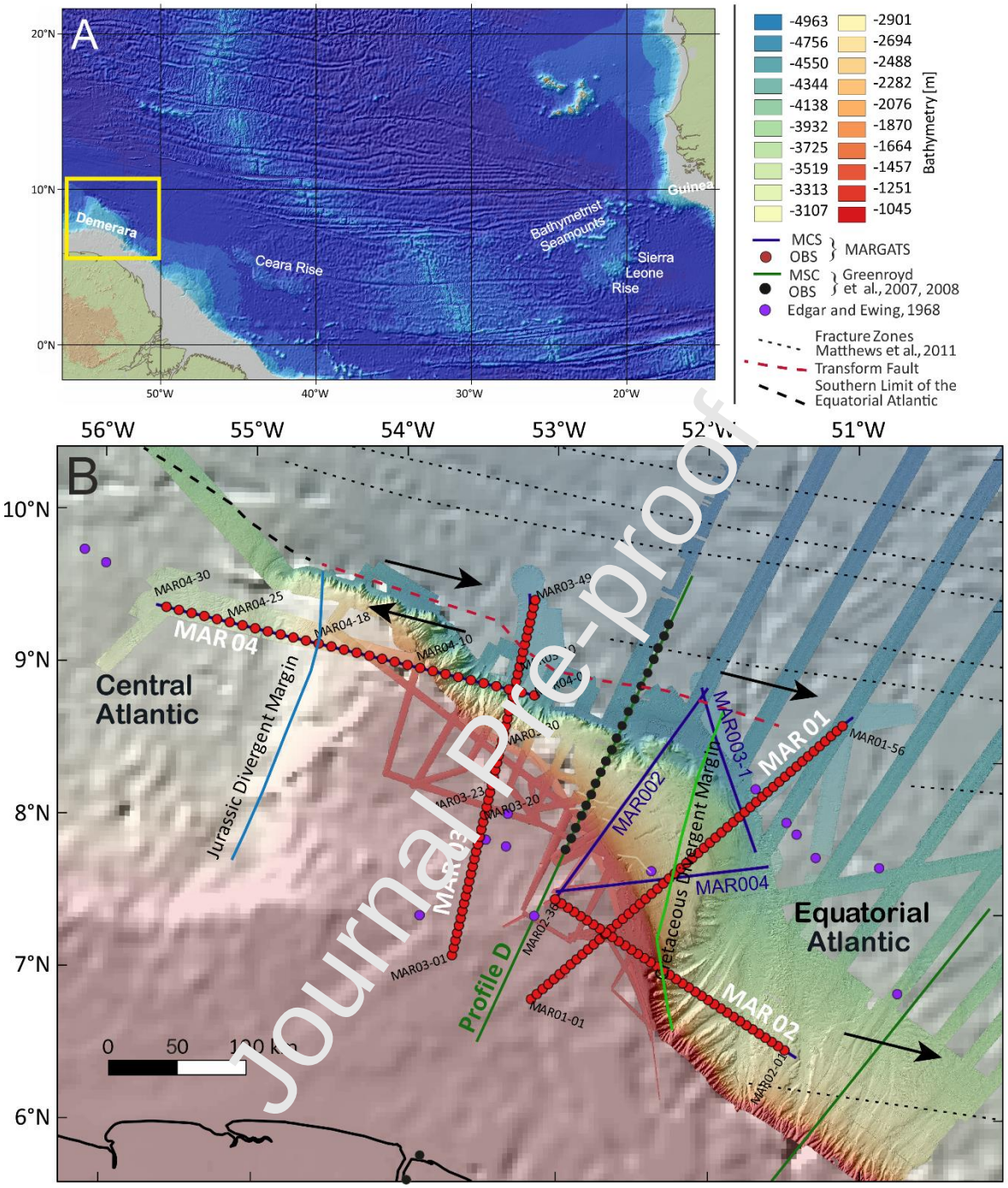

Figure 1: (A) Map of the Equatorial Atlantic, indicating structures discussed in this study. Yellow box indicates the location of the Demerara Plateau. (B) Bathymetry of the Demerara Plateau and location of the seismic profiles. OBS locations of the MARGATS cruise are marked by red dots and MCS profiles by royal blue lines. Green lines are from Greenroyd et al., 2007 and 2008 and purple dots mark the position of vintage sonobuoy deployments (Edgar and Ewing, 1968).

Later on, volcanic extrusive layers of up to 21 km thick, in the form of seaward dipping reflectors (SDRs) were identified from a network of deep-penetrating industrial seismic data (Reuber et al., 2016; Mercier de Lepinay, 2016). This led to the interpretation that large parts of the plateau are formed by magmatism, possibly related to the Bahamas Hot Spot (Reuber et al., 2016). Subsequently, based on dating dredged magmatic rocks and on plate kinematic

reconstructions, a single hotspot (the Sierra Leone hotspot) has been proposed at the origin of the magmatism of the Demerara Plateau (180-170 Ma), the Guinea plateau (165 Ma), both the Sierra Leone and Ceara Rises (76 - 68 Ma) and the Bathymetrists seamount chain (Basile et al., 2020; Figure 1).

In the eastern part of the plateau, two wide-angle seismic profiles from the MARGATS cruise (2016) (MAR01 and 02, Figure 1) imaged a narrow plateau-ocean transition zone bordering thin oceanic crust (Museur et al., 2021). At the plateau, industrial data in connection with these profiles imaged thick volcanic layers which make up the upper 15 km of the plateau, and show an underlying layer characterised by high seismic velocities (7.3-7.7 km/s), interpreted to consist of volcanic residues (Museur et al., 2021).

3 Data acquisition, methods and results

3.1 Data acquisition and quality

During the MARGATS seismic experiment (R/V L'Atalante from October 20th to November 16th, 2016, DOI: 10.17600/16001400) four regional combined Wide-Angle Seismic (WAS) and coincident seismic reflection profiles were acquired across the Demerara Plateau (Figure 1). Results from two profiles spanning the eastern plateau (MAR01 and MAR02) were presented by Museur et al. (2021). The study presented here focuses on the two unpublished wide-angle profiles located in the northwestern region of Demerara Plateau (MAR03 and MAR04, Figure 1) and their coincident seismic reflection profiles. Profile MAR04 is located along the northern edge of the Demerara Plateau between the Central and Equatorial Atlantic ocean basins. It is intersected by profile MAR03 (oriented in a N-S direction) located in the central part of the plateau. MAR03 crosses the Cretaceous transform margin in the north.

During the experiment, 49 ocean-bottom seismometers (OBS) from Ifremer (Auffret et al., 2004) were deployed along profile MAR03 (5.5 km spacing) and 30 along profile MAR04 (9.5 km spacing). All OBS recorded on three geophone channels and one hydrophone at a 4 ms sample rate. The OBS data were corrected for their time drift by comparison with GPS time before and after deployment. After data download and conversion to standard SEGY format, positions were corrected for the instrument drift from the deployment position during the descent to the seafloor using direct arrivals from the shots close to the instruments. The data quality is generally very high on all channels, especially for instruments located in deeper water, with arrivals observed with offsets up to 150 km (Figures 2 and 3) (raw data are available at: https://www.seanoe.org/data/00682/79396/).

Seismic reflection data were acquired simultaneously with the wide angle data, along all wide-angle seismic profiles and also along three additional profiles located in the north-eastern section of the plateau (Figure 1). The seismic reflection equipment from Ifremer consisted of a 3 km Sercel digital streamer with 480 channels and a tuned seismic airgun array of 6500 in^3 fired every 60 s resulting in a 150m shot spacing. The seismic reflection data were pre-processed and sorted into 6.25 m bins resulting in a 45 fold using Ifremer's "SolidQC" software. Subsequent processing on land included filtering, deconvolution, NMO correction, stacking, velocity analysis, and time migration.

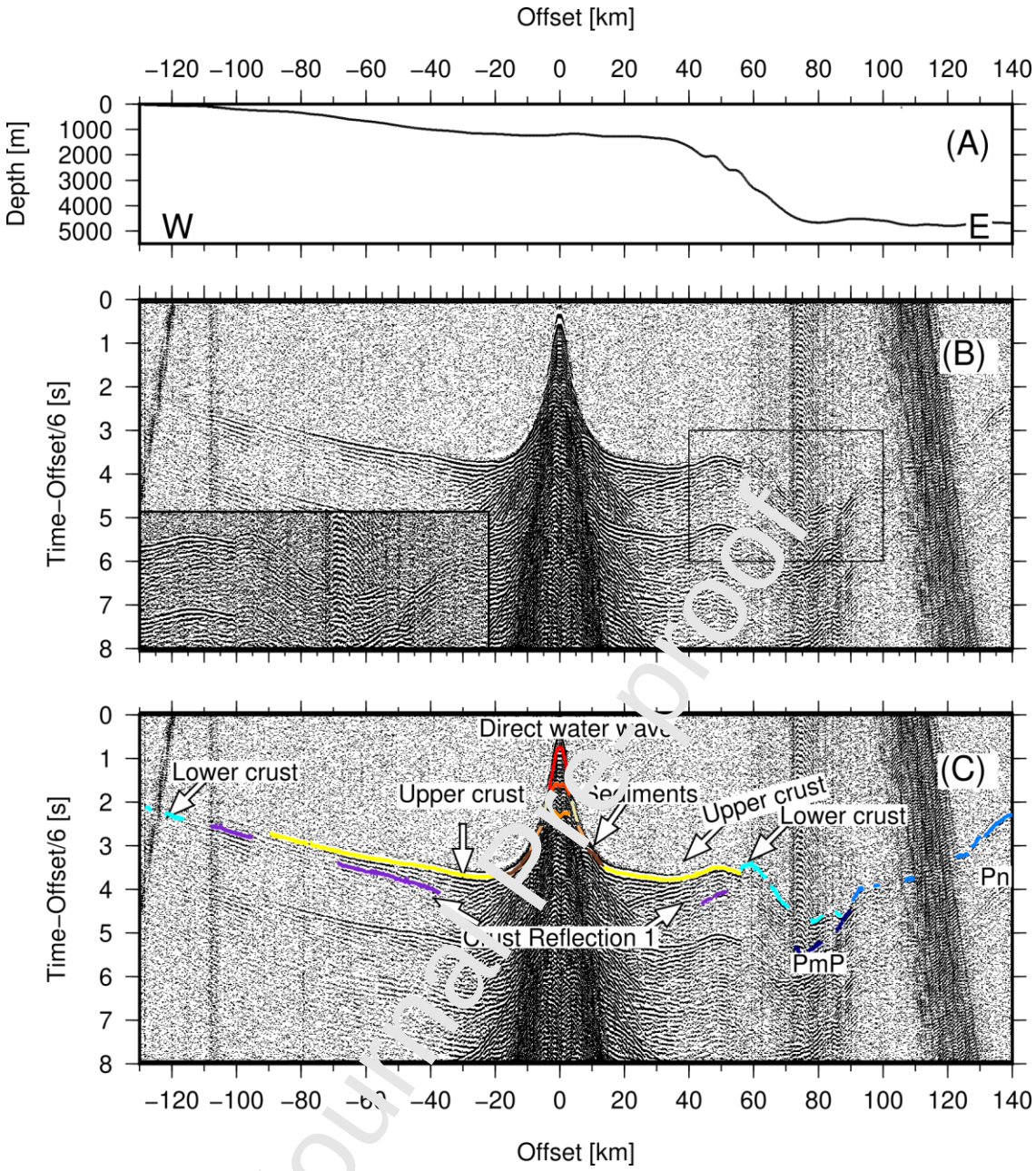

Figure 2: (a) Seafloor depth from shipboard data along the data section of profile MAR-03. (b) Bandpass filtered data of OBS MAR03-23 (location in Figure 1). Inset shows zoom indicated by black frame. (c) Bandpass filtered data (Corner frequencies 3-5-24-36 Hz) of OBS MAR03-23 with travel time picks overlain. A scale proportional to the offset has been applied and main phases are annotated. PmP = reflected rays from the Moho, Pn = turning rays from the upper mantle.

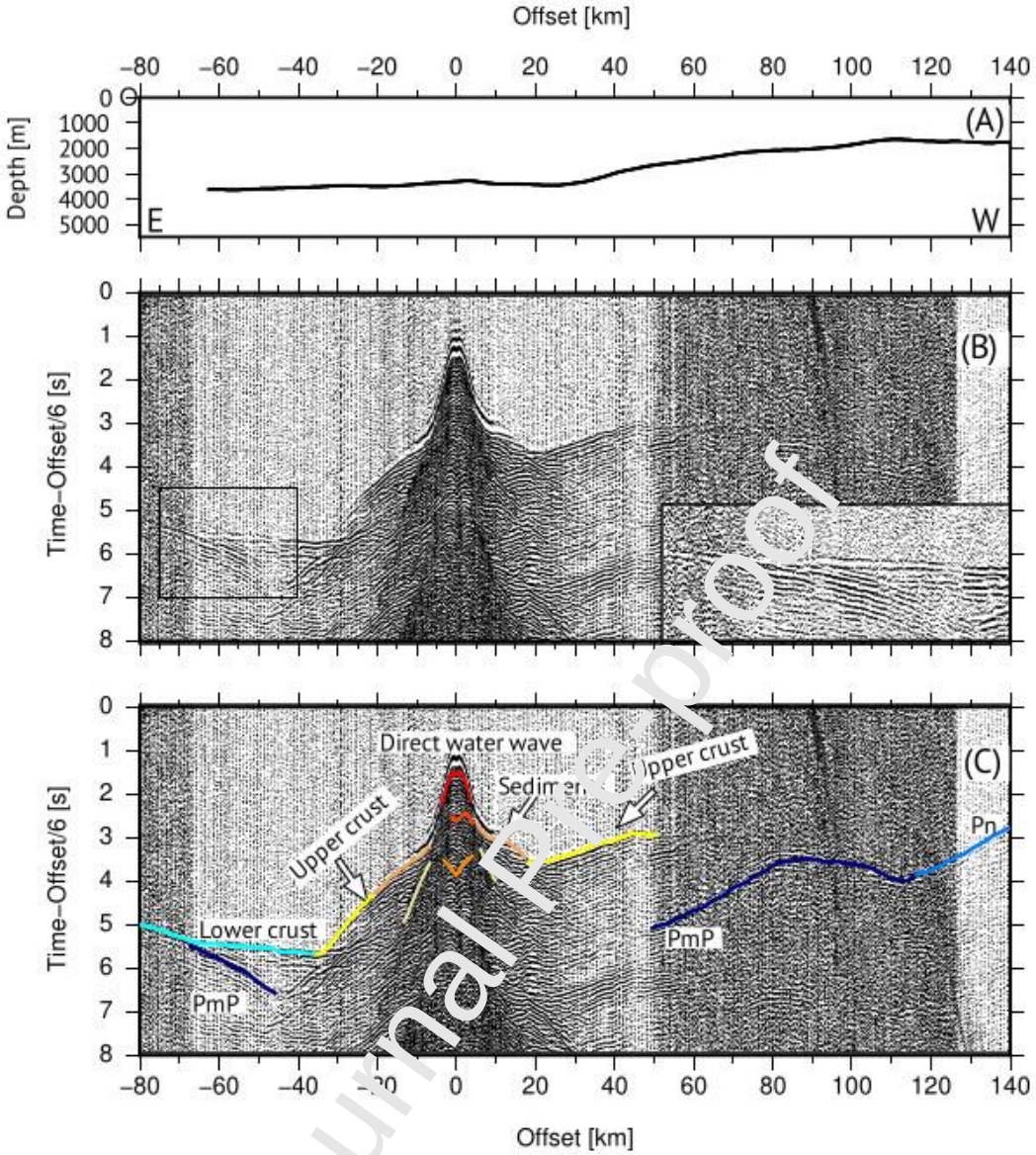

Figure 3: (a) Seafloor depth from shipboard data along profile MAR04. (b) Bandpass filtered data of OBS MAR04-18 (location in Figure 1). Inset shows zoom indicated by black frame. (c) Bandpass filtered data (*Corner frequencies 3-5-24-36 Hz) of OBS MAR04-18 with travel time picks overlain*. *A scale proportional to the offset has been applied and main phases are annotated. Pn = turning rays from the upper mantle, PmP = Reflected rays from the Moho.*

3.2 Wide-angle seismic data modeling

The wide-angle seismic data were modeled with the "*Rayinvr*" software of Colin Zelt using direct and inverse techniques (Zelt and Smith, 1992). This allows inclusion of additional information from seismic reflection and gravity data. All first and secondary P-wave arrivals were picked using the "*OpendTect*" software (dGB Earth Sciences) along the OBS sections. For the sedimentary and basement arrivals, main reflectors from the coincident seismic reflection sections were additionally picked and then converted to depth using the velocities from the seafloor instruments. A layer-stripping approach was used and the layers were

modeled from top to bottom, where shallow layers in regions unconstrained by shallow rays were adjusted to improve the fit of lower layers (Zelt, 1999). A minimum structure approach was used to avoid over-interpretation of the data (Zelt, 1999). The layer boundaries were constrained by reflections in the OBS data sections and by changes in the velocity gradients.

3.3 Error calculations

The error between the arrival times picked from the record sections and the predicted travel-time from modeling gives the first information about the overall quality of the velocity model (Figure 4 b, d, f, h and Table 1). The combined number of picks and the associated root mean square (RMS) residual errors concerning all phases are listed in Table 1.

Table 1: Summary of travel-time residuals for each phase and for the complete model for profiles MAR03 (a) and MAR04 (b). "Basement" is the Top of the Upper Crust; "PmP" is the reflection on the Moho discontinuity; "Pn" is the refracted phase in the mantle layer.

(a)

Phase name MAR03	Phase number	Number of picks	RMS Error (ms)	Chi² Error
Water	1	2406	0.041	0.170
Sediments 1	2	1061	0.127	1.619
Sediments 2	3	792	0.122	1.484
Sediments 3	9	1921	0.128	1.630
Sediments Reflection 1	4	694	0.070	0.487
Sediments Reflection 2	5	1308	0.103	1.053
Sediments Reflection 3	10	368	0.137	1.873
Basement	6	19825	0.108	1.186
Crust Reflection 1	12	1625	0.135	1.836
Lower Crust	11	5537	0.123	1.509
PmP	7	3447	0.174	3.039
Pn	8	1362	0.110	1.210
All phases		45927	0.117	1.372

(b)

Phase Name MAR04	Phase number	Number of picks	RMS Error (ms)	Chi² Error
Water	1	1391	0.040	0.167
Sediments 1	2	983	0.150	2.225
Sediments 2	3	1590	0.134	1.798
Sediments Reflection 1	4	1223	0.115	1.331
Sediments Reflection 2	5	1276	0.120	1.397
Basement	6	9678	0.116	1.537
Lower Crust	11	6187	0.118	1.866
PmP	7	4884	0.129	1.659
Pn	8	2810	0.145	2.722
All phases		30024	0.129	2.024

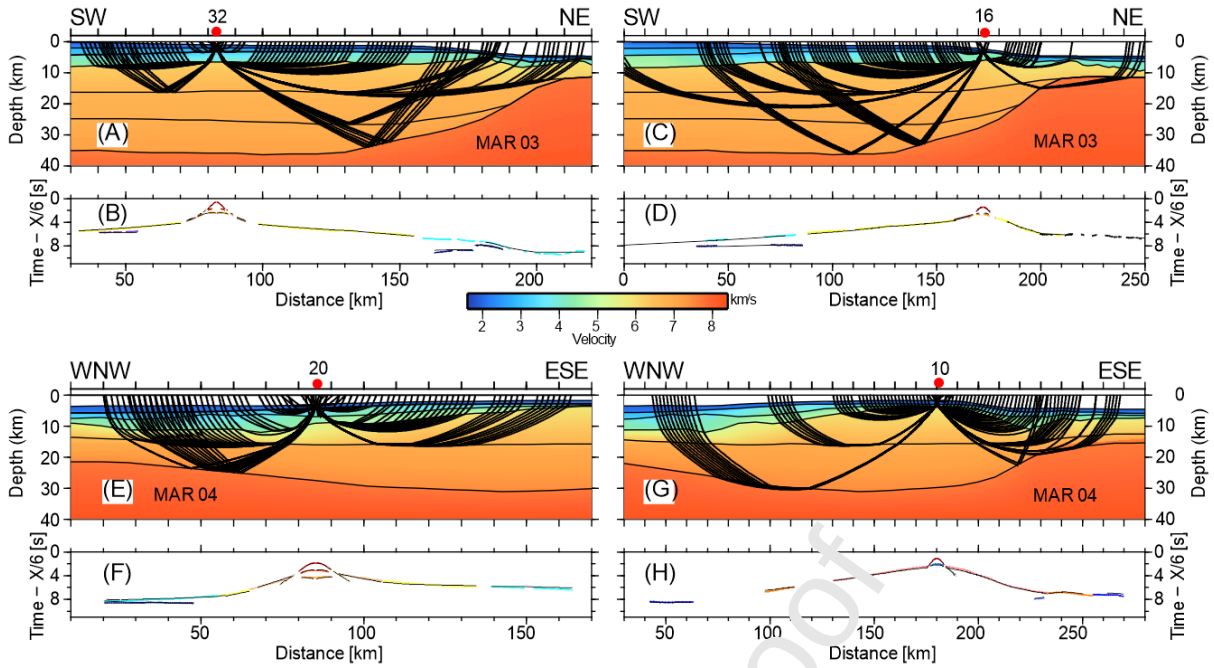

Figure 4: Model layers and ray-paths of every 10th ray (panels A, C, E, G) corresponding to travel time picks and predicted arrivals (black lines) (panels B, D, F, H) of MAR03-32 and MAR03-16 (top row), MAR04-20 and MAR04-10 (bottom row). OBS positions are marked by red circles on top.

The resolution is calculated from the number of seismic rays passing through a velocity node in the model. Therefore, it depends on the number of nodes in each layer, and gives a measure if the data are over interpreted. It presents the value of the diagonal of the resolution matrix with a maximum of one, but values less than one for nodes which do not have many rays passing. A layer without lateral velocity changes can be defined by only one velocity node through which all rays in this layer pass. This node will have a resolution of 1. Including more lateral velocity changes leading to the inclusion more nodes will decrease the percentage of rays passing each node in comparison to all rays and therefore also decrease the resolution value of each node. Typically, values greater than 0.5–0.7 indicate reasonably well-resolved model parameters (e.g. Lutter & Nowack 1990; Zelt, 1999) (see Figures 5D and 6D). However, since this is dependent on the number of rays passing through the layer, resolution values should always be considered together with hit counts, providing a measure of how well a section of the subsurface is sampled by the seismic rays (Figures 5C and 6C).

For both profiles, the resolution is high for the crustal layers and slightly less for the sedimentary layers as these are characterized by laterally variable velocities, leading to the inclusion of additional velocity nodes into the model. Model ends and the upper mantle layer show less good resolution values due to fewer rays passing to the velocity nodes.

The ray hit counts are high in the shallow layers along both profiles (> 30000), with higher values along MAR03 than MAR04 due to the denser instrument spacing. Although regions of low ray hit-count values are less well constrained, the use of the minimum structure approach (Zelt, 1999) helped to avoid over-interpretation. If a model is not well constraint, perturbations from one parameter can smear into values of neighboring velocity or depth nodes. While the variation of nodes in a well constrained region should not lead to changes in the values of the neighboring nodes, the variation of nodes in less-well constrained regions can smear into neighboring nodes. The point-spread function (SPF) gives information about the influence of velocity uncertainties spreading to neighboring nodes and, therefore, the quality of the model (Figures 5B and 6B and detailed explanation in Zelt, 1999 and Zelt and

Smith, 1992).

Taking these various error calculations into account, the depth error of the different layer boundaries should be considered to be around 0.2 km for the sedimentary layers, 0.5 km for crustal layers and up to 1 km for the deepest crustal layer and the Moho. Profile ends are seismically less well covered and the error might be higher.

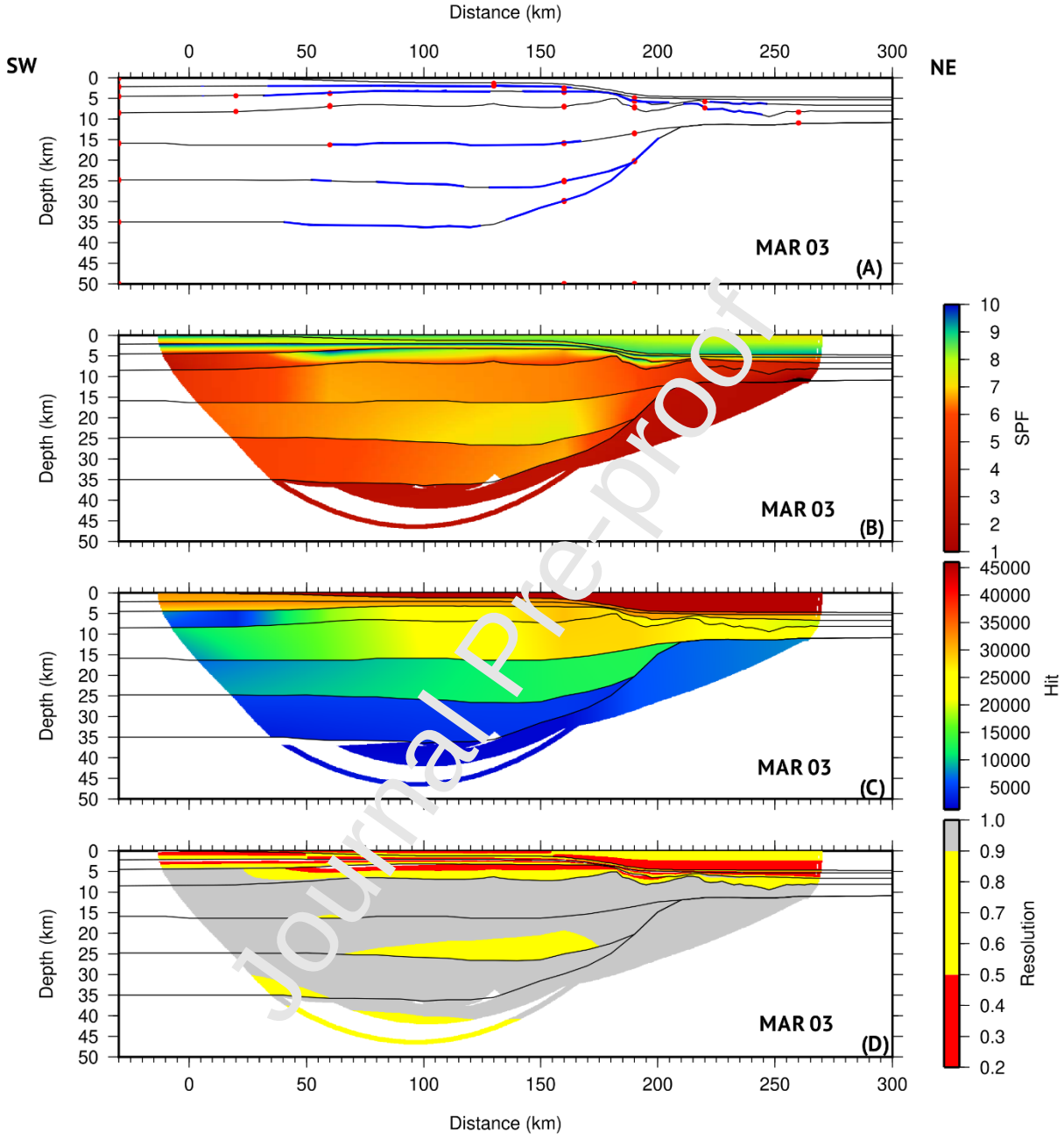

Figure 5: Error estimation of velocity model along MAR03 (A) Model parameterization including top and bottom velocity nodes (red circles) for the crustal layers. Parts of the layers constrained by reflections are highlighted in blue) (B) smearing from the spread-point function (SPF) for velocity values (C) Ray hit count (D) Resolution of velocity nodes. Zones that are not imaged by wide-angle seismic data are white.

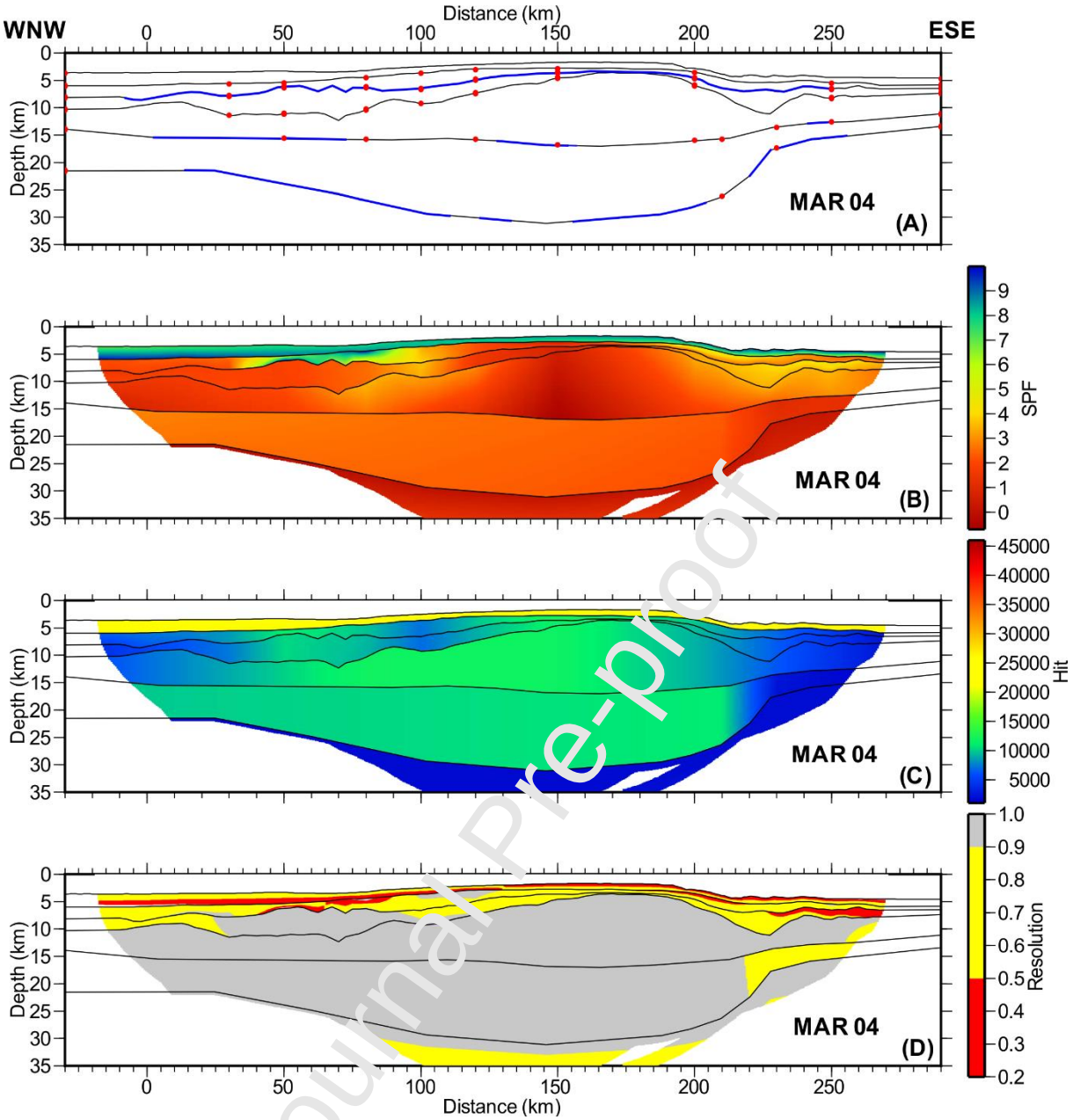

Figure 6: Error estimation of velocity model along MAR04 (A) Model parameterization including top and bottom velocity nodes (red circles) for the crustal layers. Parts of the layers constrained by reflections are highlighted in blue) (B) smearing from the spread-point function (SPF) for velocity values (C) Ray hit count (D) Resolution of velocity nodes. Zones that are not imaged by wide-angle seismic data are white.

3.4 Gravity modeling

Under the premise that the velocity model can be additionally constrained by the gravity model, we conducted gravimetric modelling using the module “Gravmod” from the “Rayinvr” software (Zelt and Ellis, 1989). This module is based on constant density trapezoids along each layer from the velocity model, associating it with an average density calculated from an empirical velocity-density relationship (Ludwig et al., 1971). In order to avoid edge effects, the model is laterally extended 30 km on both sides. For the mantle, a range of densities between 3.34 - 3.28 g / cm^3 was assumed. The calculated anomaly is compared with the observed free-air gravity anomaly derived from satellite altimetry (Sandwell & Smith, 1997). We assessed the variability of the gravity field in the vicinity of the MARGATS profiles, by

extracting two parallel profiles at 10 km distance on either side of each of them. The variability, which provides an indication of 3D effects, is represented by the grey shaded areas in Figure 7A and 7B.

- MAR03 Gravimetric Analysis:

The MAR03 profile shows four domains. Starting in the south with demain B (Figure 7A), the anomalies are positive between 0~20 mGal, and represents the central part of the plateau. Domain E is a zone of moderate crustal thinning with a 30% to 50% reduction of the anomaly to 10 mGal. Domain F shows abrupt thinning of the crust and the gravity anomalies decrease to -80 mGal, coinciding with the COB (Figure 7A). Finally, domain G shows anomalies with values around -40mGal, associated with the Equatorial Atlantic oceanic crust.

- MAR04 Gravimetric Analysis:

Along profile MAR04, five distinct domains can be identified. At the western end of the profile, domain D with anomalies around -40 mGal, marks the zone of Central Atlantic oceanic crust (Figure 7B). This is followed by domain C, where the anomaly decreases to -100 mGal: this zone coincides with the volcanic/igneous crust, 2-3 km thicker than normal oceanic crust, as described by Reuber et al. (2016). In this area, the deepening of the Moho is smooth and continuous. In the center of the profile (domain B, Figure 7B), the Moho reaches a depth of ~ 31 km. In domain E (Figure 7B), the anomaly reaches positive values of around ~30 mGal, and could be associated with volcanic materials possibly mixed with reworked continental crust, as indicated by the high-density values in the upper crust (around 2.76 g/cm^3). In domain F, the anomalies are in the order of -100 mGal. In this zone of abrupt thinning of the crust, the anomaly could be associated with the COB (Figure 7B). Finally, the anomaly increases towards the eastern end of the profile, in domain G, the values are ~ -50 mGal, associated with the Equatorial Atlantic oceanic crust.

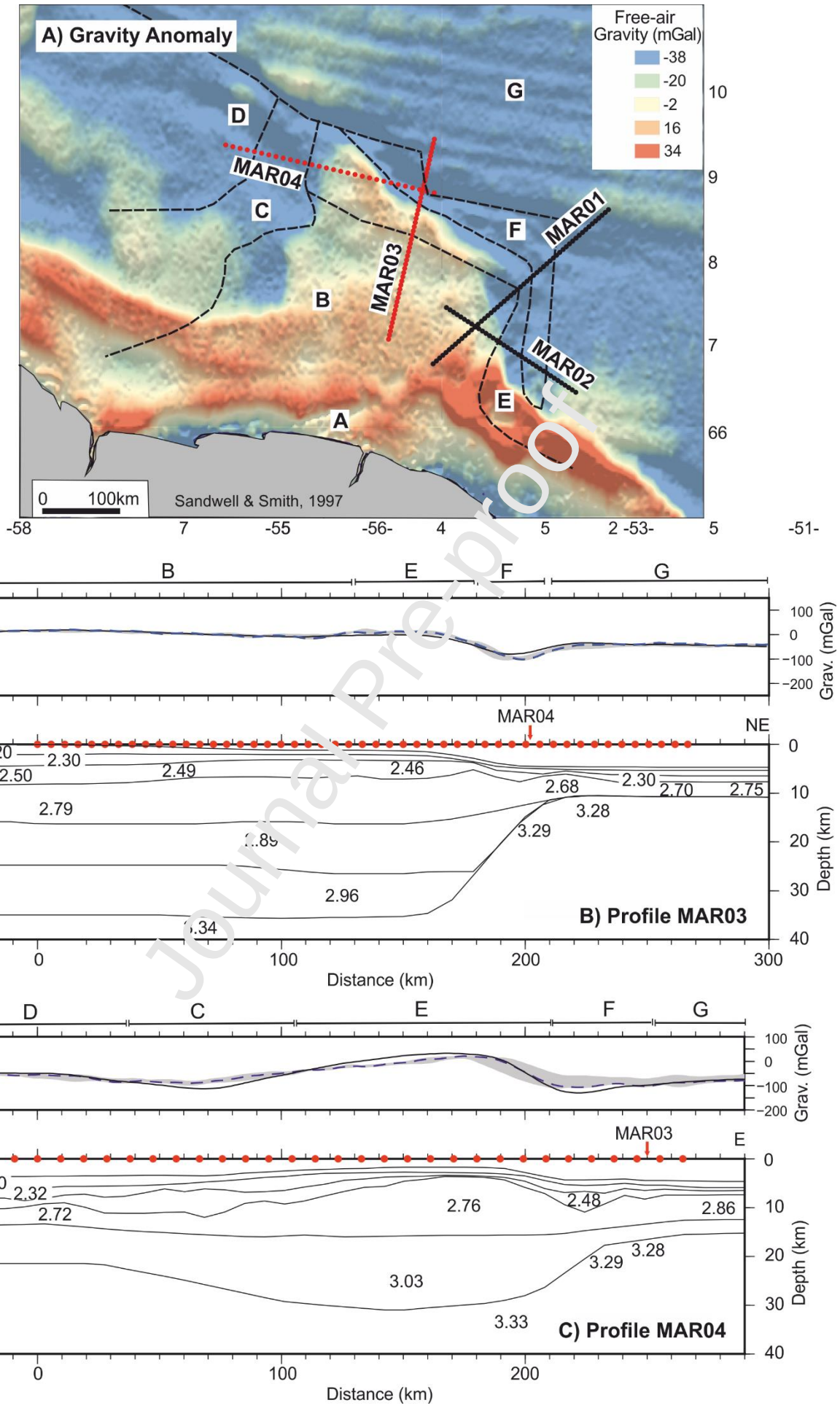

Figure 7: Results of the gravity modeling along the two transects. Italic numbers give the densities used in the model; red dots mark the horizontal positions of the OBS, and arrows the crossing point between the two profiles. The black curves illustrate the predicted gravity free-air anomaly from modeling and the dashed blue lines the observed free-air gravity anomalies (Sandwell & Smith, 1997). The grey shaded area indicates the variability of the observations in the vicinity of the profiles (see text). The different domains are indicated by the letters at the top of each panel. (A) Profile MAR03. (B) Profile MAR04.

4 Results

4.1 Wide-angle seismic models

The structure of the NW-sector of the Demerara Plateau is imaged down to 40 km in depth by the two wide-angle seismic lines, MAR03 and MAR04 (Figure 8C and D). The model obtained for MAR03 is 290 km long and includes the water layer, three shallow layers characterized by low seismic velocities, possibly corresponding to sediments, three higher velocity layers probably corresponding to either magmatic material or continental crust and the upper mantle layer. The profile MAR04, located on the northern border of the plateau, is 300 km long and includes the same layers, except the deeper lower crustal layer, which pinches out along MAR03 before reaching the crossing with MAR04. The sedimentary velocities span from 1.9 to 4.8 km/s, the underlying layers from 6.2 to 7.5 km/s and the upper mantle layer between 7.7 and 8.4 km/s.

Along MAR03, the high-velocity crustal layer thins from 26.5 km in the SW to only 3-4 km thick in the NE. In the SW, the crust is divided into 3 layers each about 9 km thick. Oceanward, the lowermost two layers pinch out, leaving a single layer crust with relatively low crustal velocities (6.0-6.5 km/s) at the northern extremity of the profile. The maximum thickness of the crustal layers along profile MAR04 is about 25.7 km at the center of the profile, slightly less than along MAR03. They thin to about 11 km towards WNW and to 6 km in the ESE. The sedimentary layers on top of the plateau are about 4-5 km thick and form up to 8 km deep sedimentary basins at the foot of the plateau. On the crust ocean ward of the plateau, the sediments are about 3-5 km thick, locally filling troughs.

While these two new profiles are imaging the deep structure of the northern and western segments of the plateau, the complementary published profiles MAR01 and MAR02 image the eastern and northeastern segment (Museur et al., 2021). The velocity models of these two profiles are also presented in Figure 8.

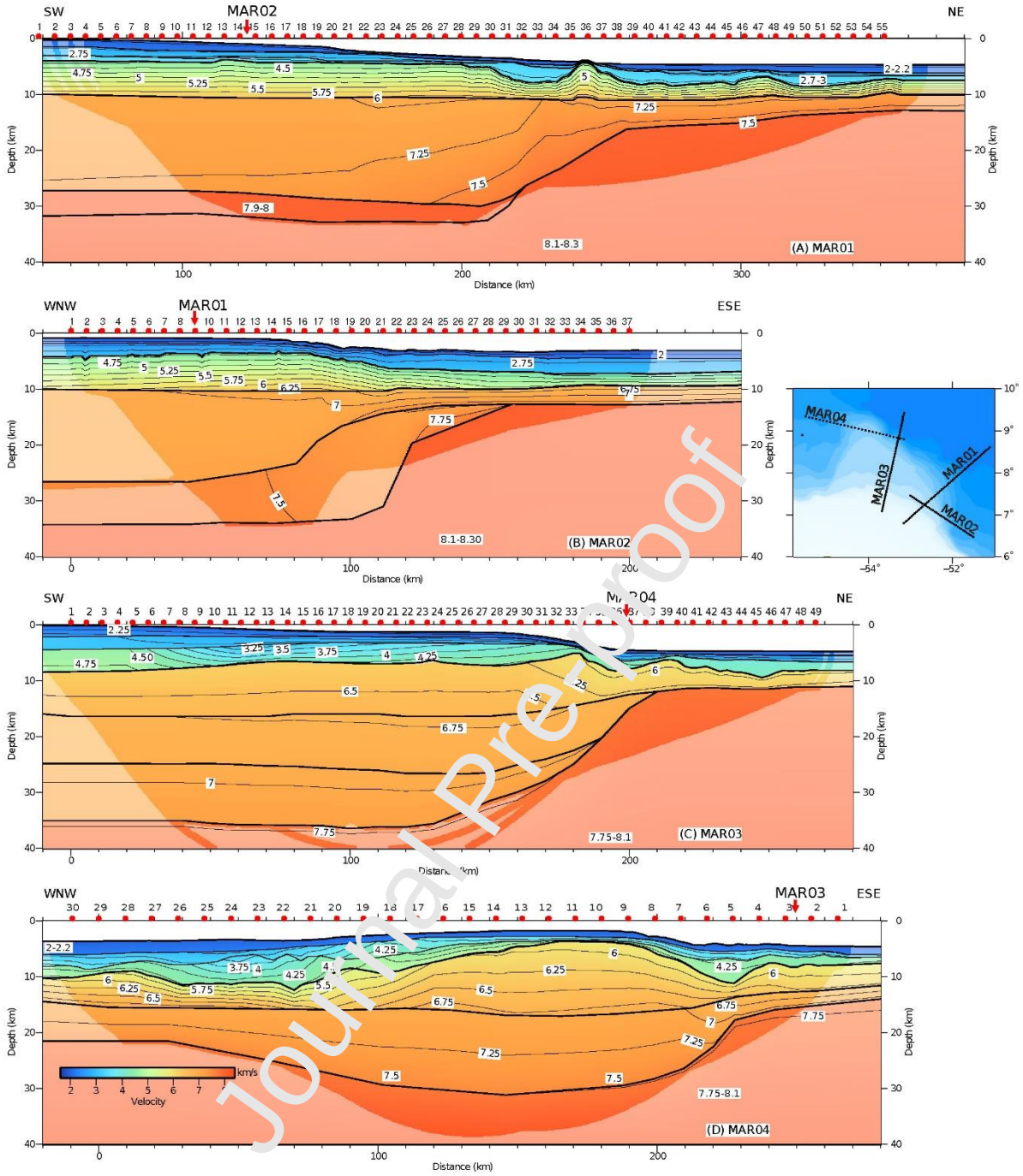

Figure 8: Wide-angle seismic models from the Demerara Plateau. The velocities are contoured every 0.25 km/s. All regions not constrained by rays from the modeling are shaded but might be constrained by the additional gravity modeling (cf. §3.6). Red dots mark the horizontal position of OBS along the profiles; all models are displayed at the same scale with a vertical exaggeration of 1:2. (A) Profile MAR01 (Museur et al., 2021) (B) Profile MAR02 (Museur et al., 2021) (C) Profile MAR03 (This study) (D) Profile MAR04 (This study). Inset shows the location of the profiles.

4.2 Comparison with MCS data sections

The velocity models are built with the help of additional information from the MCS data, and, therefore, the sedimentary layers show a good agreement between both types of seismic data (Figure 9). Integrating the most relevant seismic stratigraphic features on the MCS

profiles with the velocity model obtained from the WAS, highlights the following aspects:

From the WAS, three sedimentary packages (S1, S2 and S3), are identified in both sections (MAR03 and MAR04; Figure 9. These packages are in close agreement with the seismic stratigraphic changes along the MCS sections (Figure 9). From top to bottom, the first two packages, S1 and S2 (units in shades of blue), have velocities between 2 - 3.2 km/s, which may correspond on the plateau to the post-Albian units (e.g. Museur et al., 2021, Reuber et al., 2016; Mercier de Lépinay, 2016; Loncke et al., 2022). The reflectors are parallel to sub-parallel with strong to medium amplitudes (Figure 9A at 15-150 km; Figure 9B 100- 200 km), indicating a relatively stable depositional environment, proved to be mostly pelagic from drilled cores (Casson et al., 2021). The third sedimentary package (green unit, S3) shows a velocity range between 3.2- 5.0 km/s (), and the seismic stratigraphic expression depends on the location along the seismic lines. The high value of 5 km/s is only reached along a 20 km-wide part of velocity model MAR04 and might be due to a high amount of volcanic material in the sediments. On profile MAR04, towards the west (Central Atlantic domain), unit S3 is represented in the MCS by moderate to high amplitude semi-continuous to discontinuous reflectors, associated with Cretaceous and Jurassic faulting (Figure 9B). The central part, at the Demerara Plateau domain, represents a high amplitude content, with a tabular reflector geometry, which corresponds to an upper Jurassic-lower Cretaceous carbonate platform (Casson et al., 2021; Loncke et al., 2022). Towards the Equatorial Atlantic, at the northern end of MAR03, there is poor reflector continuity as well as variable frequency content and amplitude (Figure 9A). Figure 10 provides a zoom on this highly fractured zone, due to the Cretaceous transform/highly oblique opening of the Equatorial Atlantic ().

The top of the acoustic basement is located underneath these units and is characterised by velocities between 5.5 - 6.75 km/s (yellow/orange). Towards the Equatorial Atlantic, blocks associated with normal faulting tilting to the east can be observed (Figure 9). Towards the Central Atlantic in the MCS the sea bottom multiple does not allow to identify these types of structures.

To facilitate the further description, analyses and interpretation of the acquired data, we divided the study area in different domains, based on the different characteristics of the velocity models derived from the WAS data, including geometry and seismic velocity, as well as on gravity modelling. We define the following domains:

- Domain A represents the continental crust landward of the Demerara Plateau (not discussed here);
- Domain B represents the central part of the plateau, largely composed of SDR sequences, dipping towards the west;
- Domain C is located along the western border of the plateau and represents the transition towards the Central Atlantic;
- Domain D is the area of Jurassic oceanic crust of the Central Atlantic Ocean.
- Domain E is a zone of transition related to the opening of the Equatorial Atlantic, along the northern and eastern margins of the Demerara Plateau;
- Domain F marks a zone of abrupt transition towards the oceanic crust of the Equatorial Atlantic, and finally;
- Domain G represents the oceanic crust of the Equatorial Atlantic to the north and east of the Demerara Plateau;

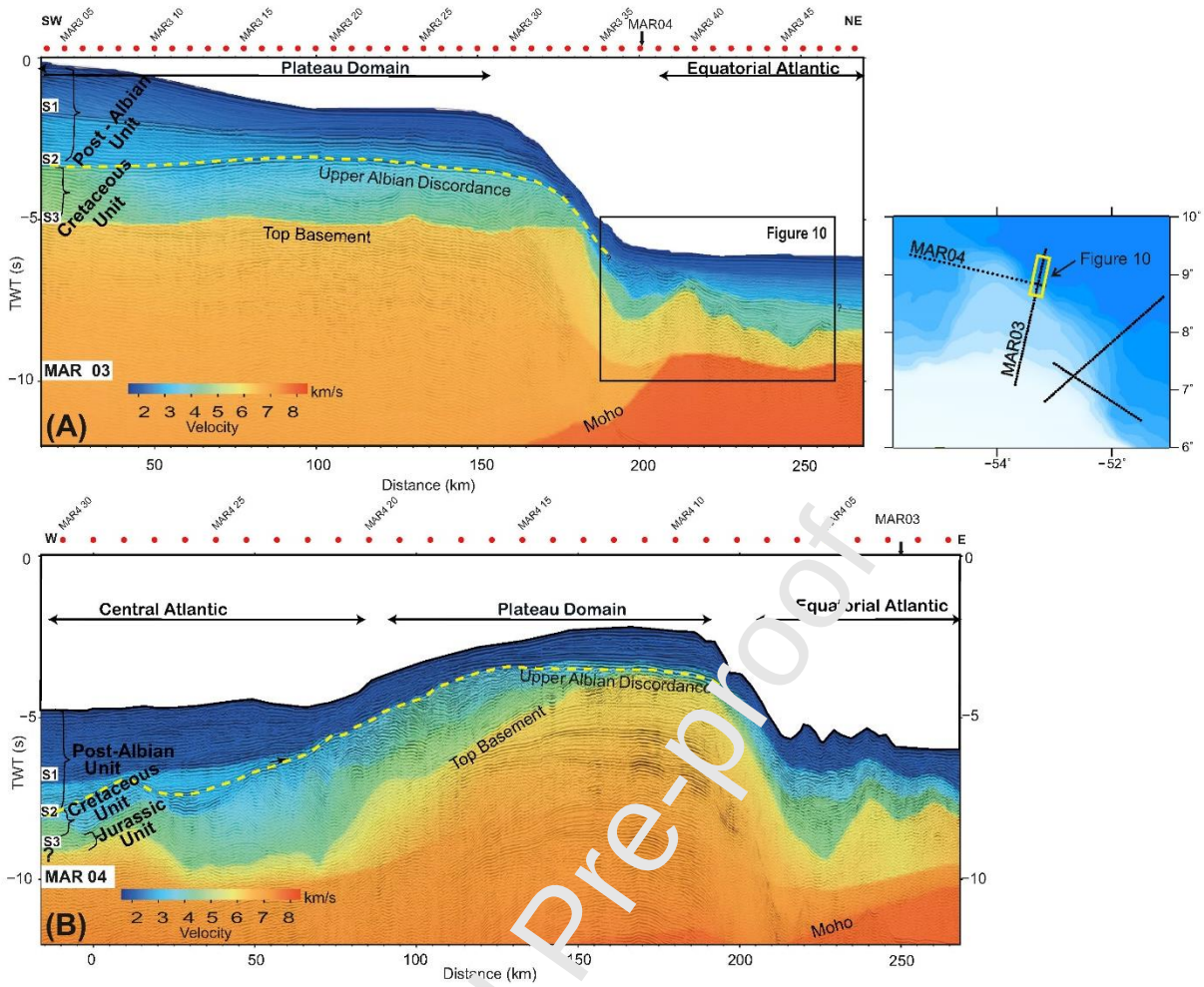

Figure 9: Seismic reflection section of (A) Profile MAR03 and (B) Profile MAR04. Underlain are the wide-angle seismic velocities and red circles depict the position of the ocean-bottom seismometers.

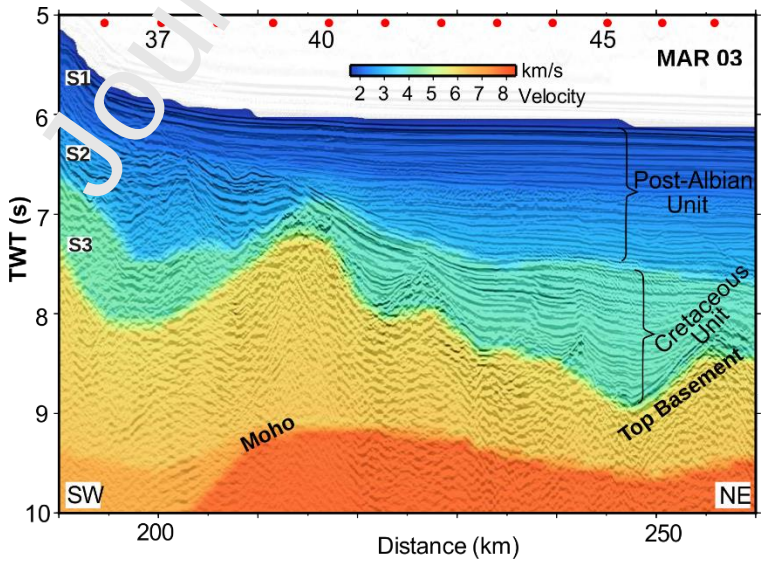

Figure 10: Zoom 1 profile MAR03. S1 and S2, sedimentary layers 1 et 2 (Post- Albian unit), respectively; S3, sedimentary layer 3 (Cretaceous unit).

5 Interpretation and discussion

In the following sections, the results from our modeling will be interpreted in terms of crustal thickness and nature. They will be compared to published seismic models from the eastern section of the plateau (Museur et al., 2021).

5.1 Profile MAR03

Along this profile, the sedimentary layers on top of the plateau are between 5-7 km thick, and undisturbed. Along the northern slope, the sedimentary section partly collapses and infills the basins at the toe of the margin (Fanget et al., 2020). Along the oceanic part of the profile, the sedimentary layers are only about 3-5 km thick. At the crossing with profile MAR4 velocities and gradients are comparable and differences lie in the error bounds (Figure 11).

This southwestern section of the Demerara Plateau is underlain by a 26.5 km thick crust (Figure 11), thinning to 3-4 km at its northern boundary over a short distance of only 80 km. It is subdivided into three distinct layers similar to continental crust as proposed by Christensen and Mooney (1992). However, as shown for the eastern section of the plateau (Museur et al., 2021), the seismic velocities are distinctively higher in the plateau than those of normal continental crust. Analogue to Museur et al., 2021, we therefore propose that a large part of the material making up the plateau is of magmatic origin, forming seaward dipping structures, more easily identifiable in the MCS sections than in the OBS data as the acoustic impedance does not change sharply between these magmatic layers (Reuber et al., 2016). The steep Moho topography along the profile MAR03 may be due to the formation of the transform margin in a shearing process at opening. The plateau-ocean transition zone is narrow, only 20-30 km wide, as compared to perpendicularly rifted margins which are often characterised by transition zones with widths of 150 to 250 km (e.g. Biari et al., 2015). The zone is marked by relatively low upper crustal velocities, probably due to fracturing and weathering during the opening. However, some highly oblique opening must have occurred as the crust displays some large blocks and thinning is gradual, especially for the lowermost layer. Thinning is observed furthest from the transition zone in the lowermost crustal layers.

A layer with velocities between 5.9 and 6.6 km/s is imaged ocean-ward of the transition zone (Figure 11). It is only 2-4 km thick, and therefore about 2-3 km thinner than typical oceanic crust (White et al., 1992). Also, the relatively high velocities in this layer are compatible with those found in regions of exhumed and serpentinised upper mantle material (Dean et al., 2000; Van Avendonk et al., 2009). Additionally, the fact that the layer is thin, does not show a separation into two sublayers and that we do not observe signs of a deep reflector corresponding to the Moho, indicates that here we might image a serpentinisation front rather than an igneous oceanic crust (Minshull et al., 1998). The top of the layer is rough, highly similar to the rough basement top found offshore Iberia and proposed to originate from upper mantle serpentinisation (Dean et al., 2000). These layers of serpentinised upper mantle material form from exhumed mantle domains of rifting before the onset of magmatic spreading (Jagoutz et al., 2007) or within the oceanic domain at slow spreading rates (Bown and White, 1994). Alternatively, this could be explained by the presence of thin oceanic crust with a thin or missing layer 3. Similar crust has been imaged at the Gakkel mid-ocean ridge in the Arctic (Jokat et al., 2003). At this ultra-slow spreading center, crustal thickness is variable between 1.4 and 3.5 km and layer 3 is completely missing. While at the magmatic centers seismic data indicate the presence of basalts of variable thickness, at the transform segments upper mantle material is exposed directly at the seafloor (Jokat et al., 2003).

Similar patches of the size of tens of kilometers of exhumed upper mantle material at the seafloor have been studied at the Southwest Indian Ridge, were continuous exhumation of mantle rocks occurred for a period of 11 Ma (Sauter et al., 2013).

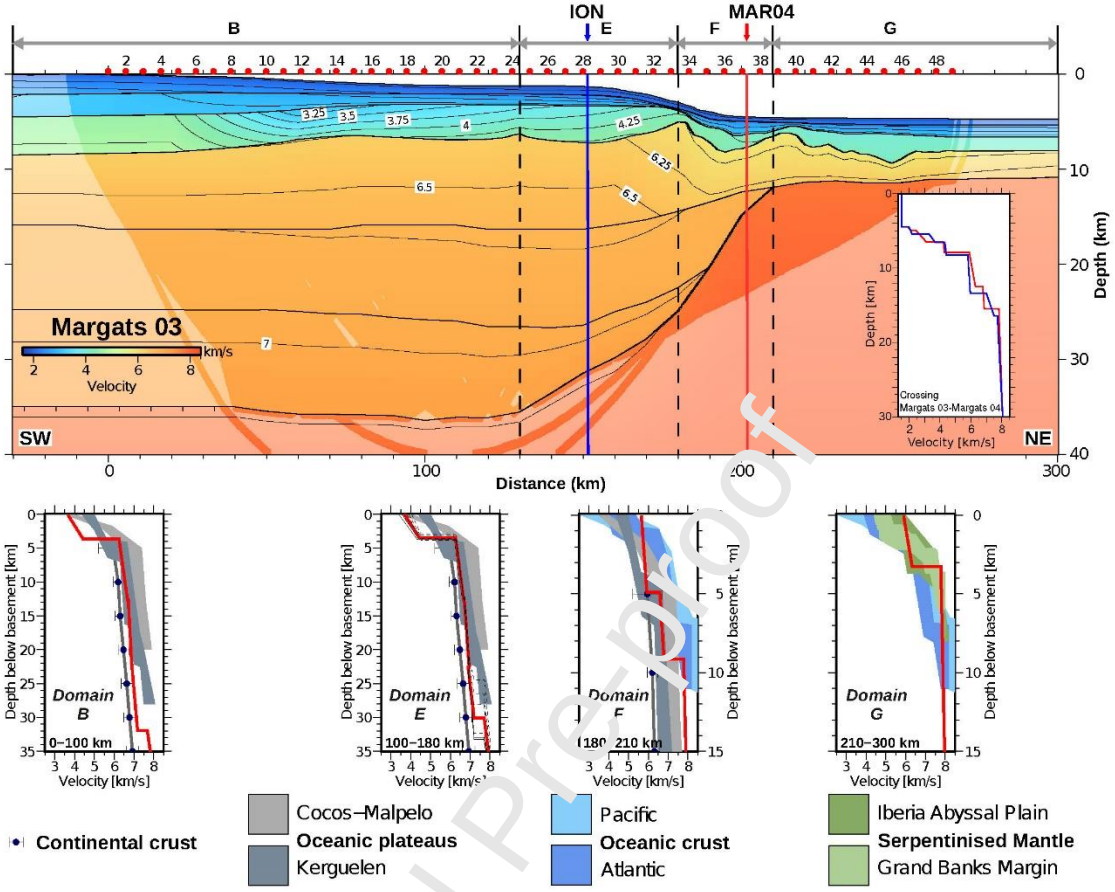

Figure 11: (Top) Final velocity model of MAR03 contoured every 0.25 km/s. Bold black lines represent layer boundaries. Inset shows Vz profiles at the crossing between MAR03 and MAR04. (Bottom) Mean Vz profiles for each of the domains crossed by profile MAR03: Domain B, between 0-130 km model distance, compared to thinned continental crust (Christensen and Mooney, 1995) and oceanic plateaus (Cocos Malpelo, Sallarès et al., (2003) and Kerguelen, Charvis et al., (1995)); Domain E, between 130-180 km model distance, also compared to thinned continental crust and oceanic plateaus; Domain F, between 180-210 km model distance, compared to thinned continental and oceanic plateau crust as well as to typical oceanic crust from the Atlantic and Pacific (White et al., 1992), and finally; domain G, between 250-290 km model distance, compared to typical oceanic crust from the Atlantic and Pacific and to serpentinised upper mantle (Van Avendonk et al., 2006; Dean et al., 2000).

5.2 Profile MAR04

Along the NW section of the plateau, profile MAR04 images both the Jurassic Central Atlantic and Cretaceous Equatorial Atlantic margins. Here, the crustal thickness reaches about 26 km at the center of the profile, thinning to 10 km toward the West and 6-7 km towards the East. At the plateau, layer thicknesses and velocities are similar to those modeled along profile MAR03 indicating the volcanic influence during the formation of the plateau (Figure 12C). While the velocities of the westernmost crust in domain D (Figure 12) fall at the border of the bounds of typical oceanic crust from White et al. (1992), its thickness

of 11-12 km is thicker than this typical crust. This could be explained by a mixture of volcanic products and early oceanic crust, produced at the creation of the margin, similar to thick crust of oceanic origin produced at oceanic plateaus. Or it could be seen as a proto-oceanic crust making the transition from a magmatic plateau to a classic oceanic crust (Chauvet et al., 2021; Sapin et al., 2021). The seismic velocities of the crust in the neighboring domain C are close to those of the plateau, indicating a similar origin as that of the rest of the plateau (Figure 12, C). Domain C shows velocities similar to those of the plateau along MAR03, with the highest lower crustal velocities at the center of the profile. This might mean that magmatic activity and thus emplacement of magmatic products increases during later development phases of the plateau. Lastly, the crust at the easternmost end of the profile shows different characteristics from the thin crust at the opposite profile end. Similar to the thin crust along MAR03, the layer thickness and velocities from our wide-angle seismic models fit to regions of serpentinised upper mantle material (Van Avendonk et al., 2006; Dean et al., 2000) or patches of thin oceanic crust from ultra-slow spreading (Jokat et al., 2007, Sauter et al., 2013). An alternative explanation, based on the analyses of seismic reflection data, is that this region belongs to the thinned crust of the plateau. The sedimentary layers thin on top of the plateau to only 2-3 km. Both slopes lead to the accumulation of sediments; however, the western basin is 8-9 km thick, about 2-3 km more than the eastern basin. The thickening of the sedimentary cover in the western side could be related to an Early Cretaceous margin-scale gravity-driven collapse (Mercier de Lépinay, 2016; Casson et al., 2021; Loncke et al., 2022).

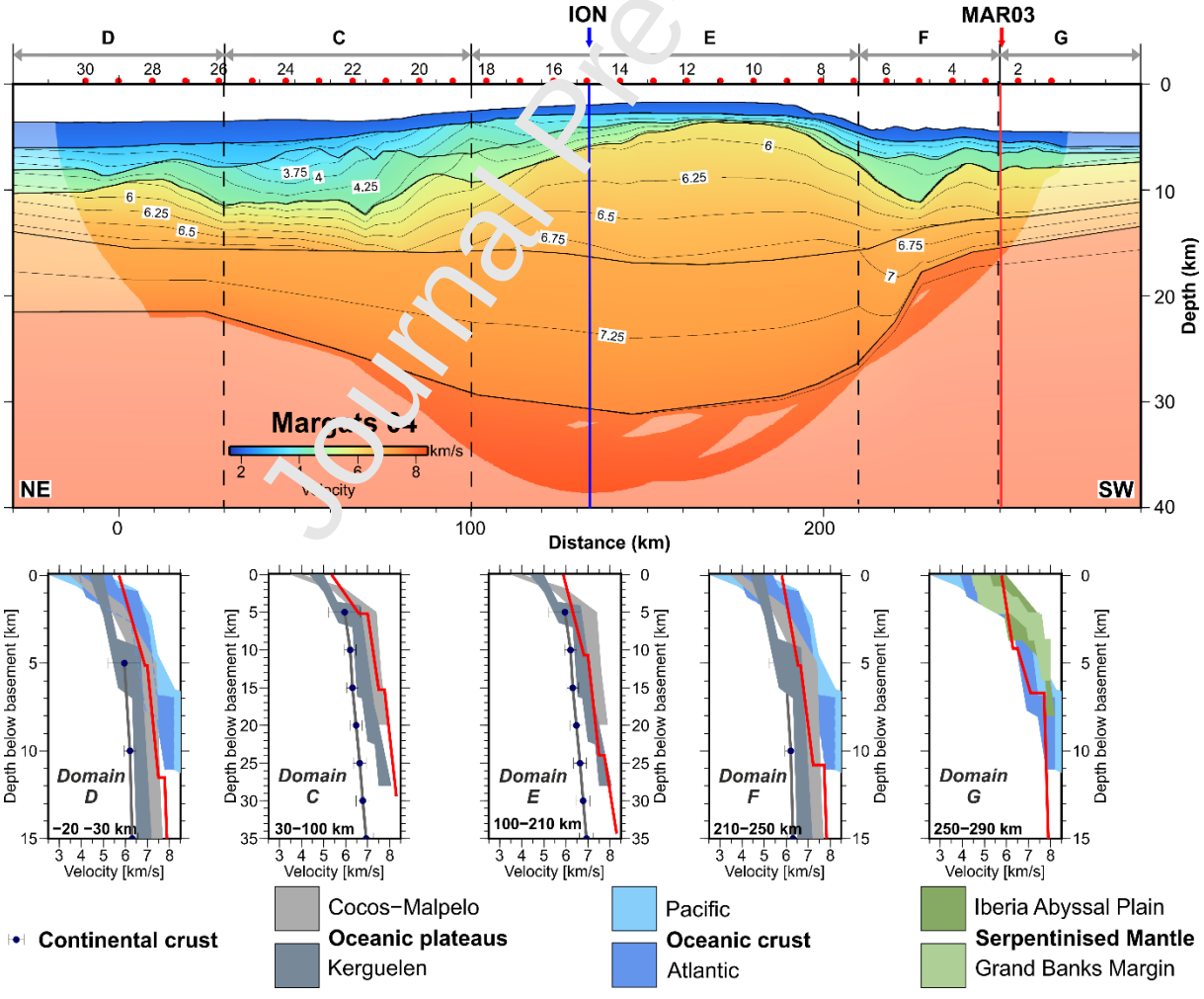

Figure 12: (Top) Final velocity model of MAR04 contoured every 0.25 km/s. Bold black lines represent layer boundaries. (Bottom) Mean Vz profiles for each of the domains crossed by

profile MAR04: Domain D, between -20 and 30 km model distance, compared to thinned continental crust (Christensen and Mooney, 1995), to oceanic plateaus (Cocos Malpelo, Sallarès et al., 2003; Kerguelen, Charvis et al., 1995) and to typical oceanic crust from the Atlantic and Pacific (White et al., 1992); Domain C, between 30 and 100 km model distance, compared to thinned continental as well as to oceanic plateau crust; Domain E, between 100 and 210 km model distance, also compared to thinned continental crust and oceanic plateau crust; Domain F, between 210-250 km model distance, compared to thinned continental crust and oceanic plateaus as well as to typical oceanic crust, and finally; Domain G, between 250-290 km model distance, compared to typical oceanic crust from the Atlantic and Pacific and to serpentinised upper mantle (Van Avendonk et al., 2006; Dean et al., 2000).

5.3 Internal structure of the Demerara Plateau

As shown above, the seismic velocities in the internal plateau are consistently higher than the mean velocity for continental crust, a fact which is in good agreement with the proposition that the plateau consists of a high percentage of volcanic material and more or less intruded continental crust (Reuber et al., 2016; Museur et al. 2021) (Figure 13). The seismic reflection data and the velocity models are in good agreement, particularly highlighting the fit of the seabed, the sedimentary packages, the top of the SDR package as well as the Moho.

Older studies of a wide-angle seismic profile sub-parallel to profile MAR03 have proposed the Demerara Plateau to consist mainly of continental crust (Greenroyd et al., 2007) (Figure 14 and sub-panels). Seaward of the plateau, oceanic crust similar to that along MAR03 is imaged with a thickness of only 3.3-5.7 km and velocities fitting to thin oceanic crust or amagmatic crust from exhumation and serpentinisation of upper mantle material. Formation of this type of amagmatic crust is observed, for example, at the ultraslow spreading Southwest Indian Ridge (Sauter et al., 2013) or in areas with important transform components. The existence of long-lived and closely-spaced transform faults might have reduced the magma supply at the time of formation of the crust or simply strongly structured the oceanic crust as in present day transforms (e.g. Van Avendonk et al., 2001)

Profiles MAR01 and MAR02 covering the eastern section of the plateau show that the internal structure of the plateau is rather homogeneous from east to west (Figure 14 b and c). A layer comprising high velocity material (P-wave velocities up to 7.5 km/s) detected along MAR02 is not imaged along MAR03 but some high velocities are found in the lower crust of MAR04. Therefore, this layer is proposed to include residual mafic material from magmatism. The oceanic crust seawards of the plateau is slightly thicker (around 5 km) than along MAR03, probably due to higher magmatism on the divergent segments at opening. The maximum Moho depth underneath the plateau is reached at MAR03 at 36.5 km and underneath the continent at 37 km along the profile of Greenroyd et al. (2007). The crustal thickness of the neighboring Guyana Shield varies between 50 km in the West and 42 km in the East (Schmitz et al., 2002; Rosa et al., 2014), which is ~5 to 15 km thicker than what is observed at Demerara Plateau (this study; Greenroyd et al., 2007).

The steep Moho geometry at the northern limit of the plateau, combined with the very narrow transition zone and absence of large tilted blocks indicate that this segment opened as a transform or highly oblique rifted margin rather than formed through margin perpendicular rifting. A basement high is located in the transition domain along profiles MAR01 and MAR03 (Figure 14B and 11, respectively). This feature is similar to the one identified by Greenroyd et al. (2007). The authors proposed it to result from either volcanic extrusives, thermal

expansion due to lateral flow of heat from young, hot, oceanic lithosphere to old, cold continental lithosphere across a transform zone (as proposed before by Gadd and Scrutton, 1997) or from density changes associated with serpentinization at the transition zone. Along profile MAR03 (Figure 11), a second basement high is observed. However, this high appears to be located on oceanic or proto-oceanic crust.

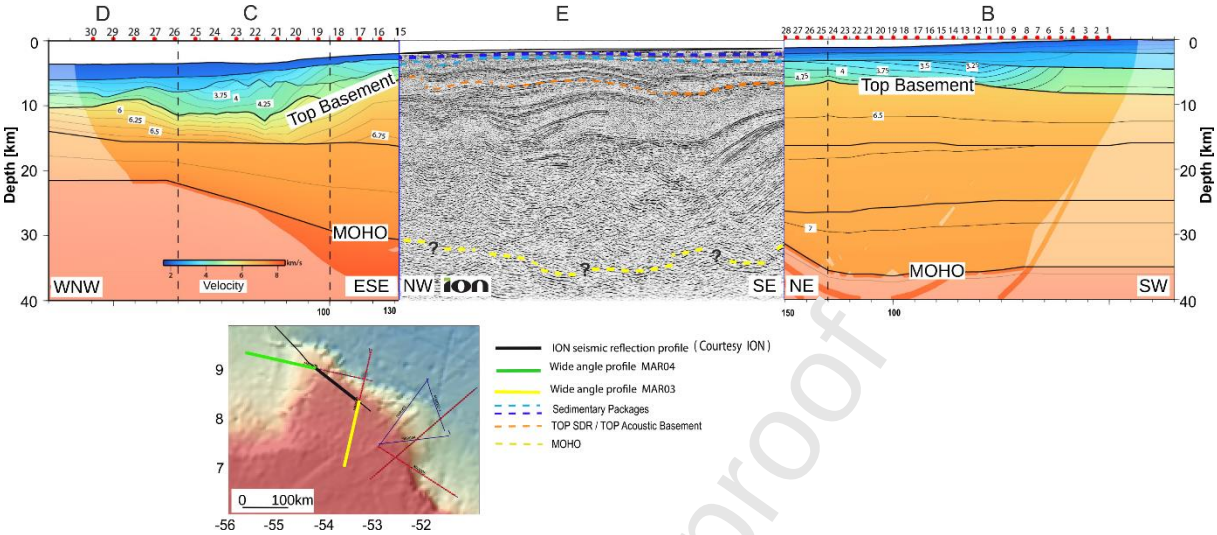

Figure 13: Composite depth image of the seismic velocity models derived from wide angle seismic profiles MAR 04 and MAR 03 combined at the intersection with the connecting depth migrated multi-channel seismic reflection profile (Seismic reflection data courtesy of ION). Inset map shows location of the three profiles

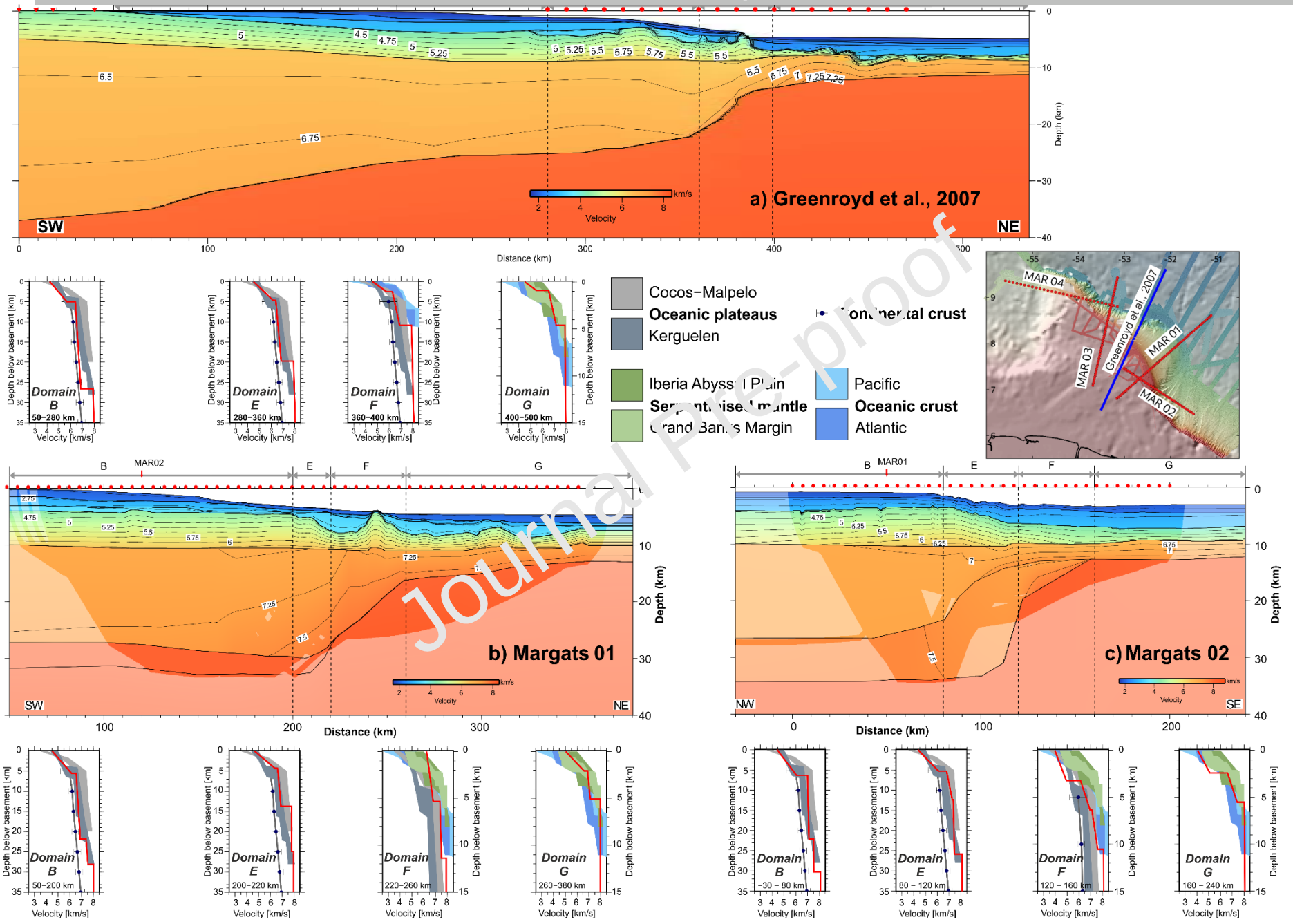

Figure 14: Final velocity models for three wide angle seismic profiles, contoured every 0.25 km/s and comparisons to published crustal types (see also the legend and captions of Figures 11 and 12). Bold black lines represent layer boundaries. (a) Final velocity model of Greenroyd et al., 2007. Lower panels show Vz-profiles for domains B, E, F and G crossed by the profile. (b) Final velocity model of MAR01 (Museur et al., 2021). Lower panels show Vz profiles for domains B, E, F and G. (c) Final velocity model of MAR02 (Museur et al., 2021). Lower panels show Vz profiles for domains B, E, F and G.

5.4 Nature of the Crust

The different data sets available for integration in this study were: a) 1D velocity-depth profiles extracted from the WAS profiles presented in this study, MAR03 and MAR04 (Figures 11 and 12), b) two profiles, MAR01 and MAR02, published by Museur et al. (2021) (Figure 14), c) the WAS profile by Greenroyd et al., 2007 (Figure 14), and d) the MCS profiles published by Reuber et al. (2016). Based on these, we propose a schematic map of spatial distribution of the nature of the crust in the study zone (Figure 15). The six different domains (B, C, D, E, F and G) defined in section 3.5 above, based on the geometry and seismic velocities derived from the WAS data and on gravity modelling, are used. They are schematically outlined in Figure 15.

Domain B covers the entire central part of the plateau domain. Along the MAR03 profile, its thickness is about 30 km at a model distance of 0-130 km. However, the measured lower crustal velocities around 7 km/s are significantly higher than those of a typical continental crust. We consider that the nature of the crust in the Demerara Plateau domain corresponds to a combination of continental crust, magmatic intrusions and SDR (Figure 13). This interpretation is analogous to those of the east of the plateau by Mercier de Lépinay (2016), Basile et al. (in press), Lesourd--Laux (2021) and to the west by Museur et al., 2021.

In domain C, located at the transition between the Plateau domain and the Central Atlantic oceanic crust further west, the thickness of the upper crust is about 5 km, with velocities of 5.5 km/s at the top and ~ 7 km/s to the base. The lower crust has a thickness of 10 km and velocities varying from top to base from 7 to 7.4 km/s, over a distance of 70 km, totaling a crustal thickness of ~15 km. This structure is similar to, but much thicker than typical oceanic crust, and the Moho is slightly rising seaward. Therefore, this domain could represent a proto-oceanic transition from the Demerara magmatic plateau to the oceanic crust, similarly to what is observed in other volcanic passive margins (Chauvet et al., 2021; Sapin et al., 2021).

Domain D corresponds to the Central Atlantic region and the thickness of the upper crust is about 5 km, with velocities ranging from 5.7 km/s at the top to ~7 km/s at the base. The lower crust has a thickness of 7 km and velocities vary from top to base from 7 to 7.4 km/s, with a total crustal thickness of ~11 km. These velocities correspond to typical oceanic crust, but the crust is much thicker than normal oceanic crust which has a 6-7 km thickness.

Domain E represents an area of similar of crustal thicknesses and velocities roughly following the equatorial transform and divergent margin segments (Figure 15). The total crustal thickness in this zone is ~25 km with top-to-bottom velocities between 6-7.5 km/s. This zone is the passage from the plateau (B) to “the abrupt transition zone” (F) that is located to the northeast.

Region F is the zone of a rather abrupt contact between the plateau domain and the Equatorial Atlantic. Over a distance of less than 40 km the total crustal thickness changes from 9 to 5 km, with top- to-bottom velocities between 5.75-7.5 km/s, which fit well with regions of exhumed and serpentinised upper mantle material (Dean et al., 2000; Van Avendonk et al., 2009), explained above (section 4.1).

Finally, in domain G, located in the Equatorial Atlantic, a gradual change in crustal thickness from the area just north of the plateau to the area further east can be observed. In the north, the layer overlying the upper mantle is about 4 km thick with velocities of 5.75 km/s at the top and ~ 6.5 km/s to the base. It differs from normal oceanic crust by the fact that it comprises only one single layer. In contrast, to the SE we observe a two-layer crust with a total thickness of ~7 km: the lower crust has a thickness of 3 km and velocities varying from 6.5 km/s to the top to 7.5 km/s at the base, and the upper crust a thickness of ~4 km and velocities ranging from 5.7 to 6.5 km/s. These values are in the range of typical oceanic crust. The change in structure and thickness between these two parts of the Cretaceous oceanic crust of the Equatorial Atlantic can be interpreted as a change of accretionary process with time, the southeastern section of profile MAR02 crossing older oceanic crust than the northern end of profile MAR 03. One can propose a decrease of magmatic input with time, maybe linked to a decreasing accretionary rate.

The integration of the analysis of 1D velocities-depth along the sections located in the study area (Figure 15) allows us to propose a schematic map of the distribution of the nature of the crust, considering the changes in crustal thickness resulting from the difference between the top of the basement and Moho depth.

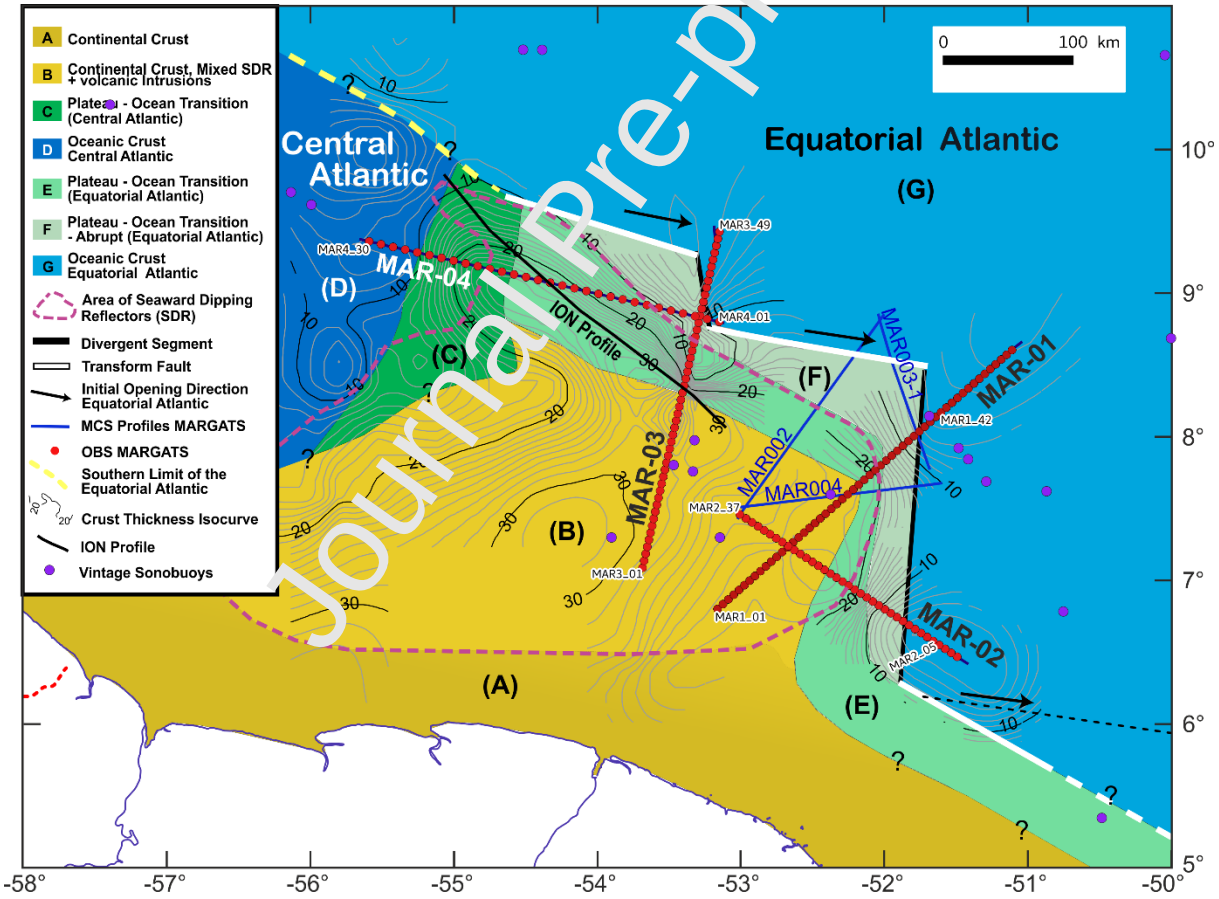

Figure 15: Schematic distribution of the crustal nature based on the data analyzed in this study. We distinguish seven domains: (A) Continental crust; (B) Combination of continental crust amalgamated with volcanic intrusions and SDRs; (C)Transition zone between the plateau and the oceanic crust to the west ; (D) Central Atlantic oceanic crust; (E) Transition zone with gradual crustal thinning, between the plateau domain and the Equatorial Atlantic oceanic crust; (F) Abrupt transition zone between the plateau and the oceanic crust of the Equatorial Atlantic; (G) Equatorial Atlantic oceanic crust.

5.5 The possible role of TMPs in the opening of the Atlantic

Numerous TMPs have been identified along passive margins (Figure 16) (Mercier de Lepinay et al., 2016; Loncke et al., 2020). These by definition include a transform margin and most of them are located at the border between oceanic basins of different ages. Up to now, five TMPs have been identified at the northern Atlantic margins and eight TMPs are located in the southern Atlantic (Mercier de Lepinay et al., 2016; Loncke et al., 2020 and references therein). Eleven of these plateaus experienced a poly-phased opening including at least one magmatic phase (Morris Jessup, Yermack, NE-Greenland, Guinea, Demerara, Sao Paulo, Walvis, Falklands-Malvinas, Hatton-Rockall, Potiguar, Aghulas), and one opened in a single magmatic phase (Vøring). Only two plateaus opened during a single phase without any volcanism (Liberia and Côte d'Ivoire-Ghana; Figure 16) (Loncke et al., 2020). However, these latter two both lack public modern seismic data coverage, which might help to distinguish between continental crust and volcanic deposits. A similar lack of data resulted in the proposition for the Demerara Plateau to be of continental nature (Greenroyd et al., 2007). The modern deep sounding data from the MARGATS cruise clearly show the magmatic influence that affected the Demerara Plateau. This is in good agreement with seismic reflection studies based on ION profiles along the plateau, showing large SDR sequences (Reuber et al., 2016). The amount of magmatic products found in this study, the fact that most TMPs have undergone magmatic phases and their location at the border of ocean basins of different ages indicate a strong relationship between rifting and the formation of TMPs.

Spreading in the Central Atlantic started at about 190 or 195 Ma, depending on the authors (e.g. Olivet, 1978; Klitgord and Schouten, 1986; Sahabi et al., 2004) with a general low obliquity of opening (Brune et al., 2018) (Figure 16). The South Atlantic opened in the south at around 140 Ma (e.g., Granot and Dyment, 2015; Chauvet et al., 2021), propagating northward. Then, the southern North Atlantic opened in two phases from south to north with final break-up around 133 Ma (e.g. Tucholke and Sibuet 2007). Later, the Equatorial Atlantic started opening 125 Ma ago as a highly oblique margin (e.g. Burke and Dewey, 1973; Sibuet and Mascle, 1978; Unternehr et al., 1988) and the full oceanic connection between the Central and North Atlantic occurred about 106 Ma ago (e.g. Pletsch et al., 2001), followed by the opening of the Labrador sea. As the last basin, the north-eastern Atlantic started rifting 55.5 Ma (Storey et al., 2007).

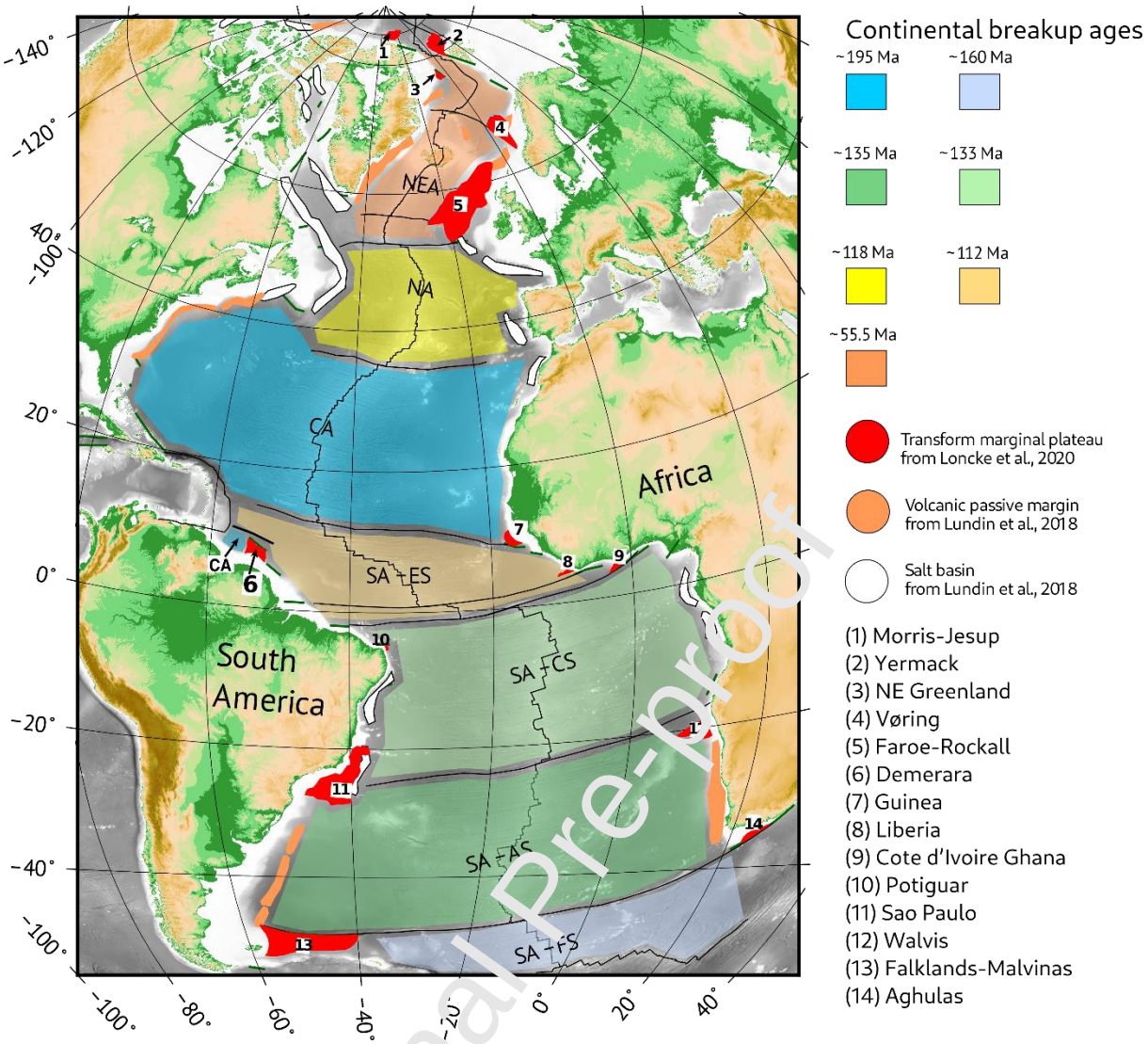

Figure 16: Location map of the Atlantic transform marginal plateaus (marked by red polygons) from Loncke et al., 2020. Orange and white polygons mark volcanic passive margins and salt basins, respectively, from Lundin et al., 2018. Transparent overlays give approximate continental breakup ages of the main oceanic basins. NEA = Northeast Atlantic, NA = North Atlantic, CA = Central Atlantic, SA-ES = South Atlantic - Equatorial Segment, SA-CS = South Atlantic – Central Segment, SA-AS = South Atlantic - Austral Segment, SA-FS = South Atlantic - Falkland Segment. Figure modified after Biari et al., 2021.

Geochemical analysis of rocks dredged from the Demerara Plateau show hotspot related magmatic origin (Basile et al., 2020). This magmatism can be explained by the presence of a previously unknown hotspot at the end of the Jurassic rifting phase underneath the Guinea and Demerara Plateau position. Using plate-reconstructions the authors propose that the hotpot was located at Sierra Leone and Ceara Rises during the upper Cretaceous oceanic spreading of the Equatorial Atlantic Ocean and that today's position of this hotspot is 100 km west of Knipovich Seamount (Basile et al., 2020). Also, hotspots seem to be involved in the formation of several of these plateaus such as the Chon Aike province (Falkland Plateau), the Etendeka-Parana Province (Santos/Walvis Plateaus) and the Iceland Hotspot (Rockall and Vøring Plateaus) (Burke et al., 1976). The existence of this hotspot can explain the geochemical composition of the plateau, however the requirement of the presence of a hotspot for the formation of the numerous TMPs along the Atlantic margins gives rise to

questions about the relationship between hotspots and marginal plateaus in general.

Volcanism during opening of an ocean basin and its rifting style are intrinsically related to each other as has been shown, for example, in the South Atlantic (Koopman et al., 2016), where the southernmost segment proposed to have rifted in a highly oblique way producing only minor volcanism. The position of TMP at the borders between ocean basins of different age, their often high magmatic content and their association to a transform margin should also be directly related to rifting processes, such as the obliquity and timing of the opening. This relationship can be explained by an alternative to the plume model, the plate model which proposes that volcanism results from lithospheric processes, with the mantle only being a passive source of melt (e. g. Foulger, 2018). It predicts that volcanism builds up in regions of lithospheric extension caused by plate tectonic forces (Foulger, 2010) and might therefore also explain the correlation between rifting and volcanism observed in TMPs. Highly oblique rifting might results in insufficient thinning and prevent sufficient adiabatic melting and therefore abundant volcanism (Koopman et al., 2016).

Rifting in ocean basins often occurs along existing weak zones, like old suture zones, as for example in the Central Atlantic (Thomas, 2019), but can also cut through cratons (e. g. East Greenland (Schiffer et al., 2015)). Rifting often starts at a segment end and propagates in one direction, as for example rifting from south to north has been proposed for the South Atlantic (Franke et al., 2007). In the Red Sea where rifting is ongoing, a compressional front proceeding the propagating rift has been observed (Bonatti and Crane, 1982). The influence of plume heads on the volcanism seems to be limited to a 200km radius in the South Atlantic (Franke et al., 2007).

When this compressional front arrives at an oblique barrier, e. g. a fracture zone, the crust can be compressively uplifted (Crane and Bonatti, 1987). Also rifting might stop when the rift arrives at a lithospheric transfer zone (Koopmann et al., 2014). A transfer zone might be a geologically inherited structure such as faults or partly ductile crustal features. This might lead to heat accumulating in the mantle and creating heavy volcanism when the rift breaks through and extends into the next segment. The accumulated heat might also cause elevated regions at the position of rift barriers (Franke, 2013). The halted rifting rifting between the opening of two ocean basins of different ages might explain the position of TMP at the border of ocean basins of different age and the abundance of magmatic products detected on most of them.

The Demerara plateau and its conjugate, the Guinea plateau, are located at the southern limit of the central Atlantic rift system. This position could have induced a heating of the underlying mantle and subsequent formation of part of the SDR complex. However, this “top-down” approach does not explain the existence of TMP without a magmatic phase nor the geochemical hotspot origin of the Demerara Plateau rocks. More detailed studies of the existence and amount of volcanism and the age and geochemical signatures of this volcanism at TMPs are clearly needed in the future.

6 Conclusions

The Demerara and its transform conjugate, the Guinea Plateau, are transform marginal plateaus, located at the border between the Central and Equatorial Atlantic ocean basins. We combined seismic velocity models with seismic reflection data from the Demerara Plateau offshore Suriname and French Guiana to define different domains associated with

the geodynamic evolution of the plateau. Our velocity models show that the plateau is underlain by thick lava flows (SDR), possibly mixed with continental crust. Underneath the Demerara Plateau, the Moho depth reaches 37 km at the border with the continent. The western border of the plateau has the characteristics of a volcanic passive margin, and the adjacent ocean crust of Jurassic age, further west, is very thick. The oceanic crust to the north of the transform margin of the plateau is very thin (2-3 km), probably due to the presence of numerous fracture zones, consistent with magma poor accretion. In the north, the seismic velocities suggest that the crust is composed to a high degree of exhumed and serpentinised upper mantle material or alternatively highly thinned plateau crust. The strong influence of magmatism during the initial formation of the plateau can be explained by either the influence of a hotspot during rifting or to mantle heating due to the rift halting at the southern border of the Central Atlantic. While the chemical composition of rocks dredged from the Demerara Plateau is in good agreement with the origin from a previously unknown hotspot underneath the plateau, the more general question of the relationship between TMPs and volcanism can be answered by a model where rifting comes to a halt at a transform, leading to the accumulation of heat in the upper mantle.

Data availability

The wide-angle seismic data in SEGY format with navigation information in the headers used in this study and plots of them will be available for download upon acceptance of the manuscript at SEANOE : https://www.seanoe.org/data/00682/79396/

Acknowledgments

The authors would like to thank the captain and the crew of R/V L'Atalante and the technical seismic teams of Genavir and Ifremer for their excellent work during the data acquisition. We also thank the PAUSE program and Ifremer for funding Crelia Padron's stay in France. The GMT (Wessel and Smith, 1995), Seismic Unix (Stockwell, 1999) and OpendTect (dGB Earth Sciences) software packages were used in the preparation of this paper. Pre-processing and quality control of the multichannel seismic data were undertaken using the SolidQC software of Ifremer. The location maps were made using the Qgis software (QGIS Development Team, 2021). We would like to acknowledge ION Geophysical for permitting the use of several deep seismic reflection profiles.

Author credits

DG and WR designed the MARGATS cruise project and obtained the funding. FK, DG, LL and CB participated in the data acquisition and initial interpretation. CP and FK modelled the wide-angle seismic data, WR the gravity data. TM modelled earlier wide-angle profiles. WR, CB, TL-L, and DG worked on the plate tectonic context of the Demerara Plateau. All authors participated in editing and improving the manuscript.

7 References

Auffret, Y., Pelleau, P., Klingelhoefer, F., Geli, L., Crozon, J., Lin, J. Y., & Sibuet, J. C. (2004).MicrOBS: A new generation of ocean bottom seismometer. first break, 22(7).

Basile, C., Maillard, A., Patriat, M., Gaullier, V., Loncke, L., Roest, W., Mercier de Lepinay, M. & Pattier, F. (2013). Structure and evolution of the Demerara Plateau, offshore French Guiana: Rifting, tectonic inversion and post-rift tilting at transform–divergent margins intersection. Tectonophysics, 591, 16-29.

Basile, C., Girault, I., Paquette, J. L., Agranier, A., Loncke, L., Heuret, A., & Poetisi, E. (2020). The Jurassic magmatism of the Demerara Plateau (offshore French Guiana) as a remnant of the Sierra Leone hotspot during the Atlantic rifting. Scientific reports, 10(1), 1-12.

Basile, C., Loncke, L., Roest, W., Graindorge, D., Klingelhoefer, F., Heuret, A., Lesourd-Laux, T., Vettel, W., Museur, T., Initiation of transform continental margins: the example of the Demerara plateau, in press, GSL special publications.

Biari, Y., Klingelhoefer, F., Sahabi, M., Aslanian, D., Schnurle, P., Berglar, K., Moulin, M., Mehdi, K., Graindorge, D., Evain, M., Benabdellouahed, M. & Reichert, C. (2015). Deep crustal structure of the North-West African margin from combined wide-angle and reflection seismic data (MIRROR seismic survey). Tectonophysics, 656, 154-174.

Biari, Y., Klingelhoefer, F., Franke, D., Funck, T., Loncke, L., Sibuet, J. C., Basile, C., Austin, J.A., Rigoti, C.A., Sahabi, M., Benabdellouahed, M., & Roest, W. R. (2021). Structure and evolution of the Atlantic passive margins: a review of existing rifting models from wide-angle seismic data and kinematic reconstruction. Marine and Petroleum Geology, 104898.

Bonatti, E., & Crane, K. (1982). Oscillatory spreading explanation of anomalously old uplifted crust near oceanic transforms. Nature, 300(5890), 343-345.

Bown, J. W., & White, R. S. (1994). Variation with spreading rate of oceanic crustal thickness and geochemistry. Earth and Planetary Science Letters, 121(3-4), 435-449.

Brune, S., Williams, S. E., and Müller, R. D. (2018). Oblique rifting: the rule, not the exception, Solid Earth, 9, 1187–1206, https://doi.org/10.5194/se-9-1187-2018.

Burke, K., & Dewey, J. F. (1973). Plume-generated triple junctions: key indicators in applying plate tectonics to old rocks. The Journal of Geology, 81(4), 406-433.

Burke, K. C., & Wilson, J. T. (1976). Hot spots on the Earth's surface. Scientific American, 235(2), 46-59.

Campan, A. (1995). Analyse cinématique de l'Atlantique équatorial: implications sur l'évolution de l'Atlantique Sud et sur la frontière de plaques Amérique du Nord/Amérique du Sud (Doctoral dissertation).

Casson, M., Jeremiah, J. et al. 2021. Evaluating the segmented post-rift stratigraphic architecture of the Guyanas continental margin. Petroleum Geoscience, 27, petgeo20202-099.http://doi.org/ 10.1144/petgeo2020-099 .

Charvis, P., Recq, M., Operto, S., & Brefort, D. (1995). Deep structure of the northern Kerguelen Plateau and hotspot-related activity. Geophysical Journal International, 122(3), 899-924.

Chauvet, F., Sapin, F., Geoffroy, L., Ringenbach, J. C., & Ferry, J. N. (2021). Conjugate volcanic passive margins in the austral segment of the South Atlantic–architecture and development. Earth-Science Reviews, 212, 103461.

Crane, K., & Bonatti, E. (1987). The role of fracture zones during early Red Sea rifting: structural analysis using Space Shuttle radar and LANDSAT imagery. Journal of the Geological Society, 144(3), 407-420.

Christensen, N. I., & Mooney, W. D. (1995). Seismic velocity structure and composition of the continental crust: A global view. Journal of Geophysical Research: Solid Earth, 100(B6), 9761-9788.

Dean, S. M., Minshull, T. A., Whitmarsh, R. B., & Louden, K. E. (2000). Deep structure of the ocean continent transition in the southern Iberia Abyssal Plain from seismic refraction profiles: The IAM-9 transect at 40 20′ N. Journal of Geophysical Research: Solid Earth, 105(B3), 5859-5885.

Edgar, T. & Ewing, J., 1968. Seismic refraction measurements on the continental margin of northeastern South America, Am. Geophys. Union, Trans., 49, 197–198.

Fanget, A. S., Loncke, L., Pattier, F., Marsset, T., Roest, W. R., Tallobre, C., Durrieu De Madron, X. & Hernandez-Molina, F. J. (2020). A synthesis of the sedimentary evolution of the Demerara Plateau (Central Atlantic Ocean) from the late Albian to the Holocene. Marine and Petroleum Geology, 114, 104195.

Foulger, G. R. (2011). Plates vs plumes: a geological controversy. John Wiley & Sons.

Foulger, G. R. (2018). Origin of the South Atlantic igneous province. Journal of Volcanology and Geothermal Research, 355, 2-20.

Franke, D. (2013). Rifting, lithosphere breakup and volcanism: Comparison of magma-poor and volcanic rifted margins. Marine and Petroleum geology, 43, 63-87.

Franke, D., Neben, S., Ladage, S., Schreckenberger, B., & Hinz, K. (2007). Margin segmentation and volcano-tectonic architecture along the volcanic margin off Argentina/Uruguay, South Atlantic. Marine Geology, 244(1-4), 46-67.

Gadd, S. A., & Scrutton, R. A. (1997). An integrated thermomechanical model for transform continental margin evolution. Geo-Marine Letters, 17(1), 21-30.

Gouyet, S., Unternehr, P., & Mascle, A. (1994). The French Guyana margin and the Demerara Plateau: geological history and petroleum plays. In Hydrocarbon and petroleum geology of France (pp. 411-422). Springer, Berlin, Heidelberg.

Gouyet, S., 1988. Évolution tectono-sédimentaire des marges guyanaise et nord-brésilienne au cours de l'ouverture de l'Atlantique sud. Ph. D. thesis, University of Pau et des Pays de l'Adour.

Graindorge, D., Museur, T., Klingelhoefer, F., Roest, W. R., Basile, C., Loncke, L., Sapin, F., Heuret, A., Perrot, J., Marcaillou, B., Lebrun, J.-F., and Déverchère, J., Deep structure of the Demerara Plateau and its two-fold tectonic evolution: from a volcanic margin to a Transform Marginal Plateau, insights from the conjugate Guinea plateau, in press, GSL special publications.

Graindorge D., Klingelhoefer F. (2016) MARGATS cruise, RV L'Atalante, https://doi.org/10.17600/16001400

Granot, R., & Dyment, J. (2015). The cretaceous opening of the South Atlantic Ocean. Earth and Planetary Science Letters, 414, 156-163.

Greenroyd, C. J., Peirce, C., Rodger, M., Watts, A. B., & Hobbs, R. W. (2007). Crustal structure of the French Guiana margin, west equatorial Atlantic. Geophysical Journal International, 169(3), 964-987.

Greenroyd, C. J., Peirce, C., Rodger, M., Watts, A. B., & Hobbs, R. W. (2008). Demerara Plateau—The structure and evolution of a transform passive margin. Geophysical Journal International, 172(2), 549-564.

Houtz, R. E., Ludwig, W. J., Milliman, J. D., & Grow, J. A. (1977). Structure of the northern Brazilian continental margin. Geological Society of America Bulletin, 88(5), 711-719.

Houtz, R. E. (1977). Sound-velocity characteristics of sediment from the eastern South American margin. Geological Society of America Bulletin, 88(5), 720-722.

Jagoutz, O., Muntener, O., Manatschal, G., Rubatto, D., Péron-Pinvidic, G., Turrin, B. D., & Villa, I. M. (2007). The rift-to-drift transition in the North Atlantic: A stuttering start of the MORB machine?. Geology, 35(12), 1087-1090.

Jokat, W., & Schmidt-Aursch, M. C. (2007). Geophysical characteristics of the ultraslow spreading Gakkel Ridge, Arctic Ocean. Geophysical Journal International, 168(3), 983-998.

Klitgord, K. D. and Schouten, H., 1986, Plate Kinematics of the Central Atlantic, in Vogt, P. R. and Tucholke, B. E., (eds.),The geology of North America v. M, The western North Atlantic region,

Geological Society of America: Decade of North American Geology, 351–378.

Koopmann, H., Brune, S., Franke, D., & Breuer, S. (2014). Linking rift propagation barriers to excess magmatism at volcanic rifted margins. Geology, 42(12), 1071-1074.

Koopmann, H., Schreckenberger, B., Franke, D., Becker, K., & Schnabel, M. (2016). The late rifting phase and continental break-up of the southern South Atlantic: the mode and timing of volcanic rifting and formation of earliest oceanic crust. Geological Society, London, Special Publications, 420 (1), 315-340.

Lesourd--Laux, T. (2020). Legacy of the Jurassic structures on the Opening of the Equatorial Atlantic; Marginal plateaux of Demerara and Guinea. Tech. rep. Total M2 internship, CSTJF (Pau).

Loncke, L., Roest, W. R., Klingelhoefer, F., Basile, C., Graindorge, D., Heuret, A., Heuret, A., Marcaillou, B., Museur, T., Fanget, A.S., & Mercier de Lépinay, M. (2020). Transform marginal plateaus. Earth-Science Reviews, 203, 102940.

Loncke, M. Mercier de Lépinay, C. Basile, A. Maillard, W.R. Roest, P. de Clarens, M. Patriat, V. Gaullier, F. Klingelhoefer, D. Graindorge, F. Sapin. Compared structure and evolution of the conjugate Demerara and Guinea transform marginal plateaus. Tectonophysics, in press, pre- proof, https://doi.org/10.1016/j.tecto.2021.229112

Ludwig, W. J., Nafe, J. E., & Drake C. L. (1971). 2. Seismic Refraction (May 1968). The Sea, Volume 4A: New Concepts of Sea Floor Evolution: Part 1, General Observations, 4, 53.

Lundin, E. R., Doré, A. G., & Redfield, T. F. (2018). Magmatism and extension rates at rifted margins. Petroleum Geoscience, 24(4), 379-392.

Lutter, W. J., & Nowack, R. L. (1990). Inversion for crustal structure using reflections from the PASSCAL Ouachita experiment. Journal of Geophysical Research, 95, 4633–4646. https://doi.org/10.1029/JB095iB04p04633

Mercier de Lepinay, M. (2016). Inventaire mondial des marges transformantes et évolution tectono-sédimentaire des plateaux de Demerara et de Guinée (Doctoral dissertation, Perpignan).

Mercier de Lépinay, M., Loncke, L., Basile, C., Roest, W. R., Patriat, M., Maillard, A., & De Clarens, P. (2016). Transform continental margins–Part 2: A worldwide review. Tectonophysics, 693, 96–115. https://doi.org/10.1016/j.tecto.2016.05.038

Minshull, T. A., Muller, M. R., Robinson, C. J., White, R. S., & Bickle, M. J. (1998). Is the oceanic Moho a serpentinization front?. Geological Society, London, Special Publications, 148(1), 71- 80.

Museur, T., Graindorge, D., Klingelhoefer, F., Roest, W. R., Basile, C., Loncke, L., & Sapin, F. (2021). Deep structure of the Demerara Plateau: From a volcanic margin to a Transform Marginal Plateau. Tectonophysics, 803, 228645.

Nemčok, M., Rybár, S., Odegard, M., Dickson, W., Pelech, O., Ledvényiová, L., Matejova, M., Molcan, M., Hermeston, S., Jones, D., Cuervo, E., Cheng, R. & Forero, G. (2016). Development history of the southern terminus of the Central Atlantic; Guyana– Suriname case study. Geological Society, London, Special Publications, 431(1), 145-178.

Olivet, J. L. (1978). Nouveau modèle d'évolution de l'Atlantique nord et central (Doctoral dissertation).

Pletsch, T., Erbacher, J., Holbourn, A. E., Kuhnt, W., Moullade, M., Oboh-Ikuenobede, F. E., Söding, E. & Wagner, T. (2001). Cretaceous separation of Africa and South America: the view from the West African margin (ODP Leg 159). Journal of South American Earth Sciences, 14(2), 147-174.

QGIS Development Team, 2021. QGIS Geographic Information System. Open Source Geospatial Foundation Project. http://qgis.osgeo.org

Reuber, Kyle R., Jim Pindell, and Brian W. Horn. "Demerara Rise, offshore Suriname: Magma-rich segment of the Central Atlantic Ocean, and conjugate to the Bahamas hot spot." Interpretation 4, no. 2 (2016): T141-T155.

Rosa, J. W. C., Rosa, J. W. C., & Fuck, R. A. (2014). Geophysical structures and tectonic evolution of the southern Guyana shield, Brazil. Journal of South American Earth Sciences, 52, 57-71.

https://doi.org/10.1016/j.jsames.2014.02.006.

Sahabi, M., Aslanian, D., & Olivet, J. L. (2004). A new starting point for the history of the central Atlantic. Comptes Rendus Geoscience, 336(12), 1041-1052.

Sallarès, V., Charvis, P., Flueh, E. R., & Bialas, J. (2003). Seismic structure of Cocos and Malpelo Volcanic Ridges and implications for hot spot ridge interaction. Journal of Geophysical Research: Solid Earth, 108(B12).

Sandwell, D. T., & Smith, W. H. (1997). Marine gravity anomaly from Geosat and ERS 1 satellite altimetry. Journal of Geophysical Research: Solid Earth, 102(B5), 10039-10054.

Sapin, F., Davaux, M. et al. 2016. Post-rift subsidence of the French Guiana hyper-oblique margin: from rift-inherited subsidence to Amazon deposition effect. From: Nemcok, M., Rybar, S., Sinha, S.T., Hermeston, S.A. & Ledvenyiova, L. (eds), Transform Margins: Development, Controls and Petroleum Systems. Geological Society, London, Special Publications, 431. http://doi.org/10.1144/SP431.11

Sapin, F., Ringenbach, J. C., & Clerc, C. (2021). Rifted margins classification and forcing parameters.Scientific Reports, 11(1), 1-17.

Sauter, D., Cannat, M., Rouméjon, S., Andreani, M., Birot, D., Bronner, A., Brunelli, D., Carlut, J., Delacour, A., Guyader, V., MacLeod, C.J., Manatschal, J., Mendel, V., Ménez, B., Pasini, V., Ruellan, E. & Searle, R. (2013). Continuous exhumation of mantle-derived rocks at the Southwest Indian Ridge for 11 million years. Nature Geoscience, 6(4), 314-320.

Schiffer C., Randell A. Stephenson, Kenni D. Petersen, Søren B. Nielsen, Bo H. Jacobsen, Niels Balling, David I.M. Macdonald; A sub-crustal piercing point for North Atlantic reconstructions and tectonic implications. Geology 2015; 43 (12): 1087–1090. https://doi.org/10.1130/G37245.1

Schmitz, M., Chalbaud, D., Castillo, J., & Izarra, C. (2002). The crustal structure of the Guayana Shield, Venezuela, from seismic refraction and gravity data. Tectonophysics, 345(1-4), 103- 118.

Sibuet, J. C., & Mascle, J. (1978). Plate kinematic implications of Atlantic equatorial fracture zone trends. Journal of Geophysical Research: Solid Earth, 83(B7), 3401-3421.

Stockwell Jr, J. W. (1999). The CWP/SU: seismic Un x package. Computers & Geosciences, 25(4), 415-419.

Storey, M., Duncan, R. A., & Tegner, C. (2007). Timing and duration of volcanism in the North Atlantic Igneous Province: Implications for geodynamics and links to the Iceland hotspot. Chemical Geology, 241(3-4), 264-281.

Thomas, W. A. (2019). Tectonic inheritance at multiple scales during more than two complete Wilson cycles recorded in eastern North America. Geological Society, London, Special Publications, 470(1), 337-352.

Tucholke, B. E., & Sibuet, J. C. (2007). Leg 210 synthesis: Tectonic, magmatic, and sedimentary evolution of the Newfoundland-Iberia rift. In Proceedings of the Ocean Drilling Program, scientific results (Vol. 210, pp. 1-56). College Station, TX: Ocean Drilling Program.

Unternehr, P., Curie, D., Olivet, J. L., Goslin, J., & Beuzart, P. (1988). South Atlantic fits and intraplate boundaries in Africa and South America. Tectonophysics, 155(1-4), 169-179.

Van Avendonk, H. J., Holbrook, W. S., Nunes, G. T., Shillington, D. J., Tucholke, B. E., Louden, K. E., Larsen, H.C. & Hopper, J. R. (2006). Seismic velocity structure of the rifted margin of the eastern Grand Banks of Newfoundland, Canada. Journal of Geophysical Research: Solid Earth, 111(B11).

Van Avendonk, H. J., Lavier, L. L., Shillington, D. J., & Manatschal, G. (2009). Extension of continental crust at the margin of the eastern Grand Banks, Newfoundland. Tectonophysics, 468(1-4), 131-148.

Van Avendonk, H. J. A., Harding, A. J., Orcutt, J. A., & McClain, J. S. (2001). Contrast in crustal structure across the Clipperton transform fault from travel time tomography. Journal of Geophysical Research: Solid Earth, 106(B6), 10961-10981.

Wessel, P., & Smith, W. H. (1995). New version of the generic mapping tools. Eos, Transactions American Geophysical Union, 76(33), 329-329.

White, R. S., McKenzie, D., & O'Nions, R. K. (1992). Oceanic crustal thickness from seismic measurements and rare earth element inversions. Journal of Geophysical Research: Solid Earth, 97(B13), 19683-19715.

Zelt, C. A. (1999). Modelling strategies and model assessment for wide-angle seismic traveltime data.Geophysical Journal International, 139(1), 183-204.

Zelt, C. A., & Ellis, R. M. (1989). Seismic structure of the crust and upper mantle in the Peace River Arch region, Canada. Journal of Geophysical Research: Solid Earth, 94(B5), 5729-5744.

Zelt, C. A., & Smith, R. B. (1992). Seismic traveltime inversion for 2-D crustal velocity structure.Geophysical journal international, 108(1), 16-34.

Declaration of interests

☒The authors declare that they have no known competing financial interests or personal relationships that could have appeared to influence the work reported in this paper.

☐The authors declare the following financial interests/personal relationships which may be considered as potential competing interests:

Author credits

DG and WR designed the MARGATS cruise projet and obtained the funding. FK, DG, LL and CB participated in the data acquisition and initial interpretation. CP and FK modelled the wide-angle seismic data, WR the gravity data. TM modelled earlier wide-angle profiles. WR, CB, TL-L, and DG worked on the plate tectonic context of the Demerara Plateau. All authors participated in editing and improving the manuscript.

Declaration of interests

☒The authors declare that they have no known competing financial interests or personal relationships that could have appeared to influence the work reported in this paper.

☐The authors declare the following financial interests/personal relationships which may be considered as potential competing interests:

Highlights

- Processing and interpretation of wide-angle and multi-channel reflection seismic data confirm the volcanic origin of the Demerara transform marginal plateau located offshore French Guiana and Surinam
- The Jurassic Central Atlantic oceanic crust located to the west of the Demerara Plateau is much thicker than normal oceanic crust
- The northern margin of the Demerara Plateau is characterised by an abrupt transition zone, typical for transform or highly oblique continental margins
- To the north of the Demerara Plateau, Equatorial Atlantic crust of Cretaceous origin is relatively thin and its velocity structure compatible with that of serpentinised upper mantle.